




# Instability of the ferromagnetic quantum critical point and symmetry of the ferromagnetic ground state in two-dimensional and three-dimensional electron gases with arbitrary spin-orbit splitting

Dmitry Miserev <sup>\*</sup>, Daniel Loss , and Jelena Klinovaja 

*Department of Physics, University of Basel, Klingelbergstrasse 82, CH-4056 Basel, Switzerland*



(Received 26 January 2022; revised 17 September 2022; accepted 19 September 2022; published 18 October 2022)

It is well known that in the absence of the spin-orbit (SO) splitting the zero-temperature ferromagnetic phase transition in two-dimensional (2D) and three-dimensional (3D) electron gas is discontinuous (first order). The physical reason for this effect lies in the infrared catastrophe brought by the long-range particle-hole fluctuations near the Fermi surface. It is widely believed that a finite SO splitting is able to regularize this infrared catastrophe, and therefore, to stabilize the ferromagnetic quantum critical point. In contrast to this, we show that the infrared catastrophe persists at arbitrary SO splitting and the zero-temperature ferromagnetic phase transition in the itinerant 2D and 3D electron gas is always discontinuous. We also find that SO splitting reduces the symmetry of the ferromagnetic ground state down to the symmetry of the spin-orbit term. For example, Rashba SO splitting in 2D electron gas leads to the easy-plane symmetry of the ferromagnetic ground state. A combination of the Rashba SO splitting with the Dresselhaus term reduces the symmetry of the ferromagnetic ground state down to the in-plane Ising ferromagnet. The infrared catastrophe can be measured via the nonanalytic dependence of the spin susceptibility on magnetic field. This dependence is strongly anisotropic and follows the symmetry of SO splitting.

DOI: [10.1103/PhysRevB.106.134417](https://doi.org/10.1103/PhysRevB.106.134417)

## I. INTRODUCTION

Itinerant ferromagnetism in two-dimensional (2D) and three-dimensional (3D) electron gas has been observed in various materials, such as manganese perovskites [1–4], transition-metal-doped semiconductors [5–7], monolayers of transition metal dichalcogenides [8–13], and many others [14–21]. The physical mechanisms leading to the ferromagnetic ground state depend strongly on the materials. Doping by transition metals results in strong interaction between the itinerant spins and the magnetic moments of the transition metal ions, the mechanism known as double exchange or Zener mechanism [22–24]. In this case, the ferromagnetism is not intrinsic but rather induced by the magnetic moments of the dopants. In contrast, in this work, we are interested in the itinerant ferromagnetism emerging from electron-electron interactions between the delocalized charge carriers. This mechanism is often referred to as the Stoner mechanism [25,26].

In the original work of Stoner [25] the phase transition to the ferromagnetic phase is of second order, i.e., continuous. The ferromagnetic quantum critical point (FQCP) of the spin-degenerate electron gas is analyzed in the literature via the effective Ginzburg-Landau-Wilson theory [27–31] describing the fluctuating magnetic order parameter. However, this theory relies on the analyticity of the effective Lagrangian [30,31], which does not hold for interacting 2D and 3D electron gases [32]. The negative nonanalytic corrections, originating from the resonant backscattering of

itinerant electrons close to the spin-degenerate Fermi surface, emerged already in second-order perturbation in the electron-electron interaction [32–40]. If these nonanalyticities survive in the vicinity of the ferromagnetic quantum phase transition (FQPT), they destabilize the FQCP at zero temperature, and lead to a first-order FQPT in 2D and 3D electron gases [33–40]. This phenomenon is an example of the fluctuation-induced first-order transition first predicted in high-energy physics [41]. In condensed matter, this effect is responsible for weak first-order metal-superconductor and smectic-nematic phase transitions [42].

The problem with FQPTs in clean metals is that it happens at very strong electron-electron interaction where the perturbative approach [32–40] is no longer valid. It was pointed out in the literature that higher-order scattering processes in the spin-degenerate electron gas [43,44] may change the sign of the nonanalytic terms making them irrelevant in the infrared limit and thus, stabilizing the FQCP. So far, the greatest advances in understanding the strongly interacting regime are attributed to the effective spin-fermion model [45] where the collective spin excitations in strongly interacting electron gases are coupled to the electron spin. The negative nonanalyticities calculated within this model remain relevant, although strongly suppressed near the FQPT [43,44].

Numerical simulations of the low-density spin-degenerate 2D electron gas (2DEG) confirm a first-order FQPT in the liquid phase with further transition to the Wigner solid at even lower densities [46–49]. The situation is less definite in a 3D electron gas (3DEG) where various advanced numerical techniques predict either a first- or second-order FQPT depending on the numerical scheme [50–55]. This disagreement between different numerical results for 3DEGs might follow from the

\*dmitry.miserev@unibas.ch

much weaker character of the nonanalytic terms destabilizing the FQCP compared to the 2D case [32].

The problem becomes even more complicated if a spin-orbit (SO) splitting of the Fermi surface is present. The main effect of the SO splitting is the spin symmetry breaking restricting possible directions of the net magnetization in the magnetically ordered phase [56,57]. In particular, the Rashba SO splitting in 2DEGs restricts possible net magnetization directions in the 2DEG plane [56,57]. So far, SO splitting is considered in the literature as a promising intrinsic mechanism cutting the nonanalyticity and stabilizing the FQCP in the interacting electron gas [58].

In this work, we consider the general case of a  $D$ -dimensional electron gas,  $D > 1$ , with arbitrary SO splitting and identify the resonant scattering processes close to the Fermi surface which result in the nonanalytic corrections with respect to the magnetization. Our results are in perfect agreement with the previously considered case of the Rashba 2DEG [56,57]. However, we show that even arbitrary SO splitting is not able to cut negative nonanalytic corrections in 2DEGs and 3DEGs. Thus, in contrast to the results of Ref. [58], we find that SO splitting cannot be considered as a possible intrinsic mechanism stabilizing FQCP in a uniform electron gas.

In this work we apply the dimensional reduction of the electron Green's function which we developed earlier in Ref. [59]. This procedure allows us to reduce  $D$  spatial dimensions to a single effective spatial dimension and significantly simplifies the derivation of the nonanalytic corrections in the perturbative regime for arbitrary SO splitting. We confirm the validity of our approach by comparison with the known results [44,56,57]. As an example, we consider 2DEG with Rashba and Dresselhaus SO splitting and find that the symmetry of the ferromagnetic ground state is broken down to the in-plane Ising ferromagnet.

The key signatures of the nonanalytic terms destabilizing the FQCP can be measured via the spin susceptibility even in the paramagnetic phase. The nonanalytic terms in the spin susceptibility are strongly anisotropic and follow the symmetry of the SO splitting. This can also be used to identify the symmetry of the SO coupling. The candidate materials for experiments are the pressure-tuned 3D metals ZrZn<sub>2</sub> [60], UGe<sub>2</sub> [61], 2D AlAs quantum wells [62], and many more, e.g., see the review in Ref. [63].

The paper is organized as follows. In Sec. II we introduce the noninteracting electron gas in  $D > 1$  spatial dimensions with arbitrary spin splitting. In Sec. III we present the asymptotics of the free electron Green's function at large imaginary time  $\tau \gg 1/E_F$  and large distance  $r \gg \lambda_F$ , where  $E_F$  is the Fermi energy and  $\lambda_F$  is the Fermi wavelength. In Sec. IV we show that the first-order interaction correction does not contribute to the nonanalyticity in the thermodynamic potential  $\Omega$ . In Sec. V we use second-order perturbation theory to derive the nonanalytic correction to  $\Omega$  with respect to arbitrary spin splitting. In Sec. VI we take the limit of small Zeeman splitting  $\mathbf{B}$  compared to the SO splitting  $\beta_{SO}$  and show that the nonanalyticity in  $\mathbf{B}$  survives at arbitrary  $\beta_{SO}$ . The nonanalytic correction is strongly anisotropic, which results in the reduced symmetry of the ferromagnetic ground state. In Sec. VII we provide an example of 2DEG with combined linear Rashba and Dresselhaus SO splittings and show that

the ferromagnetic ground state is the in-plane easy-axis (Ising) ferromagnet. In Sec. VIII we show that the nonanalytic correction to spin susceptibility in the paramagnetic (normal) phase is strongly anisotropic in the presence of the SO splitting. Directions corresponding to the maxima of spin susceptibility on the paramagnetic side of the FQPT indicate preferred directions for the net magnetization in the ordered phase. Conclusions are given in Sec. IX. Some technical details are deferred to in the Appendix.

## II. NONINTERACTING ELECTRON GAS WITH ARBITRARY SPIN SPLITTING

In this section we consider a noninteracting single-valley electron gas in  $D > 1$  spatial dimensions with arbitrary spin splitting. The case of  $D = 1$  is not included in this paper due to the Luttinger liquid instability of one-dimensional Fermi liquids with respect to arbitrarily small interactions [64]. The electron gas is described by the following single-particle Hamiltonian:

$$H_0 = \frac{p^2}{2m} - E_F - \boldsymbol{\sigma} \cdot \boldsymbol{\beta}(\mathbf{p}), \quad (1)$$

where  $\mathbf{p}$  is a  $D$ -dimensional momentum,  $m$  the effective mass,  $E_F$  the Fermi energy,  $\boldsymbol{\beta}(\mathbf{p})$  the spin splitting, and  $\boldsymbol{\sigma} = (\sigma_x, \sigma_y, \sigma_z)$  the Pauli matrices. The spin splitting is considered small compared to the Fermi energy

$$\boldsymbol{\beta}(\mathbf{p}) \equiv |\boldsymbol{\beta}(\mathbf{p})| \ll E_F, \quad (2)$$

but otherwise arbitrary. Therefore, the spin splitting close to the Fermi surface can be parametrized by the unit vector  $\mathbf{n}_p = \mathbf{p}/p$  along the momentum  $\mathbf{p}$ :

$$\boldsymbol{\beta}(\mathbf{p}) \approx \boldsymbol{\beta}(\mathbf{n}_p), \quad \mathbf{n}_p = \frac{\mathbf{p}}{p}, \quad p = k_F = \sqrt{2mE_F}. \quad (3)$$

Here we introduced  $k_F$  as the Fermi momentum at zero spin splitting  $\boldsymbol{\beta}(\mathbf{p}) = 0$ .

The eigenvectors  $|\sigma, \mathbf{n}_p\rangle$  of the Hamiltonian  $H_0$  correspond to the eigenvectors of the operator  $\boldsymbol{\sigma} \cdot \boldsymbol{\beta}(\mathbf{n}_p)$ :

$$\boldsymbol{\sigma} \cdot \boldsymbol{\beta}(\mathbf{n}_p)|\sigma, \mathbf{n}_p\rangle = \sigma \boldsymbol{\beta}(\mathbf{n}_p)|\sigma, \mathbf{n}_p\rangle, \quad (4)$$

where  $\sigma = \pm 1$  and  $\boldsymbol{\beta}(\mathbf{n}_p) = |\boldsymbol{\beta}(\mathbf{n}_p)|$ . The explicit form of the spinors is given by

$$|\sigma, \mathbf{n}_p\rangle = \frac{[\beta_-(\mathbf{n}_p), \sigma \boldsymbol{\beta}(\mathbf{n}_p) - \beta_z(\mathbf{n}_p)]^T}{\sqrt{2\boldsymbol{\beta}(\mathbf{n}_p)[\boldsymbol{\beta}(\mathbf{n}_p) - \sigma \beta_z(\mathbf{n}_p)]}}, \quad (5)$$

where the superscript  $T$  means the transposition and  $\beta_{\pm}(\mathbf{n}_p) = \beta_x(\mathbf{n}_p) \pm i\beta_y(\mathbf{n}_p)$ . Two spinors with the same  $\mathbf{n}_p$  and opposite  $\sigma$  are orthogonal

$$\langle +, \mathbf{n}_p | -, \mathbf{n}_p \rangle = 0. \quad (6)$$

This forbids the forward scattering between the bands with opposite band index  $\sigma$ .

In this paper we need the backscattering matrix elements

$$M_{\sigma\sigma'}(\mathbf{n}_p) = \langle \sigma, \mathbf{n}_p | \sigma', -\mathbf{n}_p \rangle. \quad (7)$$

Using Eq. (5), we find the matrix elements explicitly as follows:

$$M_{\sigma\sigma'}(\mathbf{n}_p) = \frac{\beta_+(\mathbf{n}_p)\beta_-(-\mathbf{n}_p) + \sigma\sigma'[\beta(\mathbf{n}_p) - \sigma\beta_z(\mathbf{n}_p)][\beta(-\mathbf{n}_p) - \sigma'\beta_z(-\mathbf{n}_p)]}{\sqrt{4\beta(\mathbf{n}_p)\beta(-\mathbf{n}_p)[\beta(\mathbf{n}_p) - \sigma\beta_z(\mathbf{n}_p)][\beta(-\mathbf{n}_p) - \sigma'\beta_z(-\mathbf{n}_p)]}}. \quad (8)$$

The spin splitting  $\beta(\mathbf{n}_p)$  results in two Fermi surfaces labeled by  $\sigma = \pm 1$  with the Fermi momenta being dependent on  $\mathbf{n}_p$ :

$$k_\sigma(\mathbf{n}_p) = \sqrt{2m[E_F + \sigma\beta(\mathbf{n}_p)]} \approx k_F + \sigma \frac{\beta(\mathbf{n}_p)}{v_F}, \quad (9)$$

where  $v_F = k_F/m$  is the Fermi velocity at  $\beta(\mathbf{n}_p) = 0$ . Here we used Eq. (2) to expand the square root.

### III. ASYMPTOTICS OF THE FREE ELECTRON GREEN'S FUNCTION

In the following it is most convenient to work with the electron Green's function in the space-time representation. In this paper we operate with the statistical (Matsubara) Green's function  $G_\sigma(\tau, \mathbf{r})$ , where  $\tau$  is the imaginary time,  $\mathbf{r}$  the  $D$ -dimensional coordinate vector, and  $\sigma = \pm 1$  the band index. In this section we present the asymptotics of the free electron Green's function  $G_\sigma^{(0)}(\tau, \mathbf{r})$  at  $\tau \gg 1/E_F$  and  $r \gg \lambda_F$ , where  $\lambda_F = 2\pi/k_F$  is the Fermi wavelength. A detailed derivation of the long-range infrared asymptotics of the Green's function is outlined in the Appendix for arbitrary geometry of the Fermi surface. Similar derivations can be found in Ref. [65] in application to the Fermi surface imaging.

The asymptotics of  $G_\sigma^{(0)}(\tau, \mathbf{r})$  at  $\tau \gg 1/E_F$  and  $r \gg \lambda_F$  comes from the sector  $(\omega, \mathbf{p})$  close to the Fermi surface:

$$\omega \ll E_F, \quad \mathbf{p} = \mathbf{k}_\sigma + \mathbf{n}(\mathbf{k}_\sigma)\delta p, \quad \delta p \ll k_F, \quad (10)$$

where  $\mathbf{k}_\sigma \in \mathcal{FS}_\sigma$  is a point on the spin-split Fermi surface  $\mathcal{FS}_\sigma$  with index  $\sigma$ ,  $\mathbf{n}(\mathbf{k}_\sigma)$  is the outward normal at this point,  $\delta p > 0$  ( $\delta p < 0$ ) corresponds to empty (occupied) states at zero temperature, see Fig. 5(a). The free electron Green's function  $G_\sigma^{(0)}(i\omega, \mathbf{p})$  is given by the quasiparticle pole

$$G_\sigma^{(0)}(i\omega, \mathbf{p}) \equiv G_\sigma^{(0)}(i\omega, \delta p, \mathbf{n}) = \frac{|\sigma, \mathbf{n}\rangle\langle\sigma, \mathbf{n}|}{i\omega - v_\sigma(\mathbf{n})\delta p}, \quad (11)$$

where we shortened  $\mathbf{n}(\mathbf{k}_\sigma)$  to  $\mathbf{n}$  here,  $|\sigma, \mathbf{n}\rangle$  is the spinor given by Eq. (5),  $v_\sigma(\mathbf{n})$  is the Fermi velocity at  $\mathbf{k}_\sigma$ . Here we also linearized the dispersion with respect to  $\delta p$  because  $\delta p \ll k_F$ . At the same time, the finite curvature of the Fermi surface is important for the asymptotic form of  $G_\sigma^{(0)}(\tau, \mathbf{r})$ .

Here we consider nearly spherical Fermi surfaces with small deformations coming from the spin splitting, see Eq. (9). In this case the asymptotic expansion of the free-electron Matsubara Green's function contains two terms, see Eq. (A49),

$$G_\sigma^{(0)}(\tau, \mathbf{r}) \approx \left(\frac{1}{\lambda_F r}\right)^{\frac{D-1}{2}} \left[ e^{i(k_\sigma(\mathbf{n}_r)r - \vartheta)} g_\sigma^{(0)}(\tau, r, \mathbf{n}_r) + e^{-i(k_\sigma(-\mathbf{n}_r)r - \vartheta)} g_\sigma^{(0)}(\tau, -r, -\mathbf{n}_r) \right], \quad (12)$$

$$\mathbf{n}_r = \frac{\mathbf{r}}{r}, \quad \vartheta = \frac{\pi}{4}(D-1),$$

$$g_\sigma^{(0)}(\tau, x, \mathbf{n}) = \int_{-\infty}^{\infty} \frac{d\delta p}{2\pi} e^{i\delta p x} G_\sigma^{(0)}(\tau, \delta p, \mathbf{n}) = \frac{1}{2\pi} \frac{|\sigma, \mathbf{n}\rangle\langle\sigma, \mathbf{n}|}{ix - v_F \tau}, \quad (13)$$

where  $k_\sigma(\mathbf{n})$  is given by Eq. (9) for arbitrary unit vector  $\mathbf{n}$ ,  $\lambda_F$  is the Fermi wavelength,  $v_F = k_F/m$  is the Fermi velocity at zero spin splitting, and  $\mathbf{n}_r = \mathbf{r}/r$  is the unit vector along  $\mathbf{r}$ . Here we stress that Eq. (12) is true only if the SO splitting is small compared to  $E_F$ , see Eq. (2). We also neglected the weak dependence of the Fermi velocity on the spin splitting in Eq. (13),  $v_\sigma \approx v_F$ , because it does not provide any non-analyticities. We see from Eq. (12) that the Green's function contains the oscillatory factors that are sensitive to the spin splitting through  $k_\sigma(\pm\mathbf{n}_r)$ , see Eq. (9). As we will see later, these oscillatory factors are responsible for the nonanalytic terms in the thermodynamic potential  $\Omega$ . The dimensional reduction of the electron Green's function for spherical Fermi surfaces is covered in Ref. [59].

### IV. FIRST-ORDER INTERACTION CORRECTION TO $\Omega$

In this and the following sections we calculate the non-analytic corrections to the thermodynamic potential  $\Omega$  in the limit of weak electron-electron interaction. The calculation is performed within first- and second-order perturbation theory. Our results extend existing theories [33–35,44,56] to the case of arbitrary spin splitting. In particular, we show that arbitrary SO splitting is not able to gap out all soft fluctuation modes and the nonanalyticity in  $\Omega$  with respect to the magnetic field  $\mathbf{B}$  survives, in contrast to the predictions of Ref. [58]. As we are only after the nonanalytic terms in  $\Omega$ , all analytic corrections will be dropped.

Let us start from the first-order interaction correction to  $\Omega$ , see Fig. 1(a):

$$\Omega^{(1)} = \frac{1}{2} \sum_{\sigma, \sigma'} \int dz V_0(z) P_{\sigma\sigma'}(z), \quad (14)$$

$$P_{\sigma\sigma'}(z) = -\text{Tr}\{G_\sigma^{(0)}(z)G_{\sigma'}^{(0)}(-z)\}, \quad (15)$$

where  $z = (\tau, \mathbf{r})$ , Tr stands for the spin trace, and  $P_{\sigma\sigma'}(z)$  is the particle-hole bubble. Here,  $V_0(z)$  is the Coulomb interaction,

$$V_0(\tau, \mathbf{r}) = \frac{e^2}{\epsilon r} \delta(\tau), \quad (16)$$

where  $e$  is the elementary charge,  $\epsilon$  the dielectric constant, and  $\delta(\tau)$  is due to the instantaneous nature of the Coulomb interaction (the speed of light is much larger than the Fermi velocity). Using the asymptotics of the Green's function  $G_\sigma^{(0)}(\tau, \mathbf{r})$ , see Eq. (12), we find the asymptotics of the particle-hole

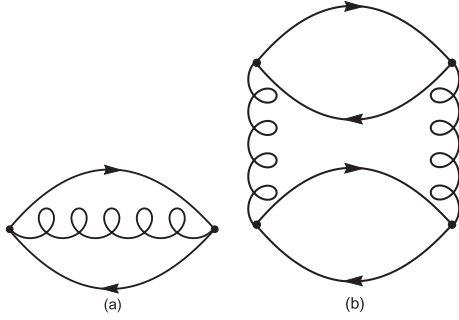


FIG. 1. (a) First-order interaction correction to  $\Omega$ , see Eq. (14). (b) Second-order interaction correction to  $\Omega$  contributing to the nonanalyticity. Solid lines correspond to the electron propagators  $G_{\sigma\sigma'}^{(0)}(\tau, \mathbf{r})$ , see Eq. (12); wiggly lines stand for the Coulomb interaction, see Eq. (16).

bubble

$$P_{\sigma\sigma'}(\tau, \mathbf{r}) = P_{\sigma\sigma'}^L(\tau, \mathbf{r}) + P_{\sigma\sigma'}^K(\tau, \mathbf{r}), \quad (17)$$

$$P_{\sigma\sigma'}^L(\tau, \mathbf{r}) \approx \frac{\delta_{\sigma\sigma'}}{2\pi^2} \left( \frac{1}{\lambda_F r} \right)^{D-1} \frac{v_F^2 \tau^2 - r^2}{(r^2 + v_F^2 \tau^2)^2}, \quad (18)$$

$$P_{\sigma\sigma'}^K(\tau, \mathbf{r}) \approx \frac{1}{4\pi^2} \frac{1}{r^2 + v_F^2 \tau^2} \left( \frac{1}{\lambda_F r} \right)^{D-1} \times [e^{-2i\vartheta} e^{ir(k_\sigma(\mathbf{n}_r) + k_{\sigma'}(-\mathbf{n}_r))} |M_{\sigma\sigma'}(\mathbf{n}_r)|^2 + e^{2i\vartheta} e^{-ir(k_\sigma(-\mathbf{n}_r) + k_{\sigma'}(\mathbf{n}_r))} |M_{\sigma\sigma'}(-\mathbf{n}_r)|^2], \quad (19)$$

where the matrix elements  $M_{\sigma\sigma'}(\pm\mathbf{n}_r)$  are given by Eq. (8). Here  $P_{\sigma\sigma'}^L(\tau, \mathbf{r})$  is the Landau damping contribution to the particle-hole bubble coming from the forward scattering. It is clear that this contribution is insensitive to the spin splitting. The second contribution,  $P_{\sigma\sigma'}^K(\tau, \mathbf{r})$ , is the Kohn anomaly coming from the backscattering with the momentum transfer close to  $2k_F$ . The Kohn anomaly is sensitive to the spin splitting through the oscillatory factors containing the Fermi momenta  $k_\sigma(\pm\mathbf{n}_r)$ , see Eq. (9).

As only the Kohn anomaly is sensitive to the spin splitting  $\beta(\mathbf{n}_p)$ , we can simplify Eq. (14):

$$\Omega^{(1)} = \frac{1}{2} \sum_{\sigma, \sigma'} \int_{S_{D-1}} d\mathbf{n}_r \int_0^\infty dr r^{D-1} \frac{e^2}{\epsilon r} P_{\sigma\sigma'}^K(0, \mathbf{r}), \quad (20)$$

where  $S_{D-1}$  is the  $(D-1)$ -dimensional unit sphere,  $d\mathbf{r} = r^{D-1} dr d\mathbf{n}_r$ . The integral over  $r$  is divergent at small  $r$  (the ultraviolet divergence) because it takes the following form:

$$\int_0^\infty \frac{dr}{r^3} e^{ir\Delta} \rightarrow \infty, \quad (21)$$

where  $\Delta$  is either equal to  $\Delta = k_\sigma(\mathbf{n}_r) + k_{\sigma'}(-\mathbf{n}_r)$  or to  $\Delta = -k_\sigma(-\mathbf{n}_r) - k_{\sigma'}(\mathbf{n}_r)$ . This divergence comes from the asymptotics of the particle-hole bubble, see Eq. (19), that is only valid at  $r \gg \lambda_F$ . Therefore, the lower limit for  $r$  in Eq. (21) is bounded by  $r \sim \lambda_F$ . This divergence can also be cured via the analytical continuation to the Euler gamma function  $\Gamma(x)$  using the following identity:

$$I_\alpha(\Delta) = \int_0^\infty \frac{dr}{r^\alpha} e^{ir\Delta} = \frac{\pi |\Delta|^{\alpha-1}}{\sin(\pi\alpha)\Gamma(\alpha)} e^{-i\frac{\pi}{2}(\alpha-1)\text{sgn}(\Delta)}. \quad (22)$$

In our case  $\alpha = 3$  and the integral is indeed divergent due to  $\sin(3\pi) = 0$  in the denominator. Therefore, we consider  $\alpha = 3 + \delta$  and take the limit  $\delta \rightarrow 0$ :

$$\int_0^\infty \frac{dr}{r^3} e^{ir\Delta} = \frac{\Delta^2}{2} \left( \frac{1}{\delta} + \ln|\Delta| - i\frac{\pi}{2} \text{sgn}(\Delta) \right). \quad (23)$$

Now it is clear that the physical dimension of  $\Delta$  under the logarithm has to be compensated by the ultraviolet scale  $p_0 \sim 2k_F$ , which is equivalent to cutting the lower limit in Eq. (21) at  $r \sim \lambda_F$ :

$$\int_{\sim\lambda_F}^\infty \frac{dr}{r^3} e^{ir\Delta} = \frac{\Delta^2}{2} \left( \ln \left| \frac{\Delta}{p_0} \right| - i\frac{\pi}{2} \text{sgn}(\Delta) \right). \quad (24)$$

We subtracted out the divergent terms originating from  $r \sim \lambda_F$  because they do not contribute to the nonanalyticity in the spin splitting due to the infrared long-range nature of the nonanalytic corrections. However, this can be seen explicitly. The term  $\sim 1/\lambda_F^2$  that is not present in Eq. (24) does not depend on  $\Delta$  and can be safely subtracted out. The linear term  $\sim \Delta/\lambda_F$ , which is also not present in Eq. (24) is analytic (no absolute value is taken), and thus, it cannot contribute to any nonanalyticity. One can explicitly substitute it back into Eq. (20) and check that any term linear in spin splitting disappears after the summation over the spin indices. Now, we come back to  $\Omega^{(1)}$  where  $\Delta$  is either equal to  $\Delta = k_\sigma(\mathbf{n}_r) + k_{\sigma'}(-\mathbf{n}_r)$  or to  $\Delta = -k_\sigma(-\mathbf{n}_r) - k_{\sigma'}(\mathbf{n}_r)$ , so using Eq. (9) we find

$$|\Delta| \approx 2k_F + \frac{\sigma\beta(\pm\mathbf{n}_r) + \sigma'\beta(\mp\mathbf{n}_r)}{v_F}. \quad (25)$$

As the spin splitting is much smaller than the Fermi energy, we can expand the logarithm  $\ln|\Delta/p_0|$  in the analytic Taylor series with respect to the spin splitting. Hence, we see that  $\Omega^{(1)}$  does not contain any nonanalyticities for arbitrary spin splitting.

Here we performed the calculations for the long-range Coulomb interaction Eq. (16). Finite electron density results in the Thomas-Fermi screening of the long-range Coulomb tail on the scale of the screening length  $r_0$ . The weak coupling limit that we consider in this section corresponds to  $r_0 \gg \lambda_F$ . However, the integral over  $r$  in  $\Omega^{(1)}$  converges at  $r \sim \lambda_F \ll r_0$  because  $\Delta \approx 2k_F$  here. Therefore, we can indeed neglect the Thomas-Fermi screening in this section.

## V. SECOND-ORDER INTERACTION CORRECTIONS TO $\Omega$

We see from the calculation of  $\Omega^{(1)}$  that the nonanalytic terms may come from the oscillatory integrals like the one in Eq. (22). However, we have to subtract the  $2k_F$  factor first, such that  $\Delta$  in Eq. (22) becomes proportional to the spin splitting. One way to achieve this is to consider  $\Omega^{(1)}$ , see Eq. (14), with the interaction  $V(\tau, \mathbf{r})$ , which has oscillatory components  $e^{\pm i2k_F r}$ . In fact, the electron-electron interaction acquires such components upon the dynamic screening by the particle-hole bubble. One consequence of this is the Thomas-Fermi screening, which we already discussed and concluded that it is not important if the interaction is weak. However, there is another much more important consequence of such dressing that results in  $2k_F$  harmonics in the interaction due to

backscattering of electrons near the Fermi surface, the effect known as Friedel oscillations. As we consider the correlations at large  $r \sim v_F/\beta \gg \lambda_F$ , where  $\beta$  is a characteristic value of the spin splitting at the Fermi surface, the interaction matrix elements at the momentum transfer  $2k_F$  are effectively local, so we can use the effective contact interaction

$$V_{2k_F}(z) = u \delta(\mathbf{r})\delta(\tau) = u \delta(z), \quad (26)$$

$$u \approx V_0(2k_F) = \frac{2\pi^{\frac{D}{2}} \Gamma(D-1)}{\Gamma(\frac{D}{2})} \frac{e^2}{\epsilon(2k_F)^{D-1}}, \quad (27)$$

where  $\delta(\mathbf{r})$  is the  $D$ -dimensional delta function and  $V_0(q)$  is the Fourier transform of the Coulomb interaction Eq. (16).

$$P_{\sigma_1\sigma_2}(z)P_{\sigma_3\sigma_4}(z) = \frac{e^{ir\Delta_{\sigma_3\sigma_4}^{\sigma_1\sigma_2}(\mathbf{n}_r)} |M_{\sigma_1\sigma_2}(\mathbf{n}_r)M_{\sigma_3\sigma_4}(-\mathbf{n}_r)|^2 + e^{-ir\Delta_{\sigma_3\sigma_4}^{\sigma_1\sigma_2}(-\mathbf{n}_r)} |M_{\sigma_1\sigma_2}(-\mathbf{n}_r)M_{\sigma_3\sigma_4}(\mathbf{n}_r)|^2}{(2\pi)^4(\lambda_F r)^{2(D-1)}(r^2 + v_F^2\tau^2)^2} \dots, \quad (30)$$

$$\Delta_{\sigma_3\sigma_4}^{\sigma_1\sigma_2}(\mathbf{n}_r) = k_{\sigma_1}(\mathbf{n}_r) + k_{\sigma_2}(-\mathbf{n}_r) - k_{\sigma_3}(-\mathbf{n}_r) - k_{\sigma_4}(\mathbf{n}_r) \approx \frac{(\sigma_1 - \sigma_4)\beta(\mathbf{n}_r) + (\sigma_2 - \sigma_3)\beta(-\mathbf{n}_r)}{v_F}, \quad (31)$$

where the dots in Eq. (30) stand for the rapidly oscillating terms on the scale of  $2k_F$  and  $4k_F$  and also the forward scattering contribution, which does not contain any nonanalytic dependence on the spin splitting. We used Eq. (9) to express  $\Delta_{\sigma_3\sigma_4}^{\sigma_1\sigma_2}(\mathbf{n}_r)$  in terms of the spin splitting.

Then we substitute Eq. (30) into Eq. (29) and evaluate the integral over  $z = (\tau, \mathbf{r})$ . The integral over  $\tau$  is elementary

$$\int_{-\infty}^{\infty} \frac{d\tau}{(r^2 + v_F^2\tau^2)^2} = \frac{\pi}{2v_F r^3}. \quad (32)$$

The integral over  $r$  can be represented using the integral  $I_\alpha(\Delta)$  defined in Eq. (22)

$$\Omega^{(2)} = -\frac{u^2}{2^6\pi^3 v_F \lambda_F^{2(D-1)}} \sum_{\sigma_i} \int_{S_{D-1}} d\mathbf{n}_r \times |M_{\sigma_1\sigma_2}(\mathbf{n}_r)M_{\sigma_3\sigma_4}(-\mathbf{n}_r)|^2 \text{Re}\{I_{D+2}[\Delta_{\sigma_3\sigma_4}^{\sigma_1\sigma_2}(\mathbf{n}_r)]\}, \quad (33)$$

where  $\text{Re}$  stands for the real part. Here we used that  $I_\alpha(-x) = I_\alpha^*(x)$ , where the star corresponds to the complex conjugation.

At this point it is convenient to introduce the dimensionless interaction parameter  $g$ :

$$g = uN_F = \frac{umk_F^{D-2}}{2^{D-1}\pi^{\frac{D}{2}}\Gamma(\frac{D}{2})}, \quad (34)$$

where  $N_F$  is the density of states per band at the Fermi level. Substituting Eq. (27) into Eq. (34), we find an estimate for the dimensionless coupling constant  $g$ :

$$g \approx \frac{\Gamma(D-1)}{2^{2D-3}\Gamma^2(\frac{D}{2})} \frac{1}{k_F a_B}, \quad a_B = \frac{\epsilon}{me^2}, \quad (35)$$

If we dress the interaction line in Fig. 1(a) by a single particle-hole bubble, we get the second-order diagram for  $\Omega$  shown in Fig. 1(b)

$$\Omega^{(2)} = -\frac{1}{4} \sum_{\sigma_i} \int d z_1 d z_2 d z_3 V_{2k_F}(z_2) V_{2k_F}(z_3 - z_1) \times P_{\sigma_1\sigma_2}(z_1) P_{\sigma_3\sigma_4}(z_3 - z_2). \quad (28)$$

Using the contact approximation Eq. (26), we simplify  $\Omega^{(2)}$  to the following expression:

$$\Omega^{(2)} = -\frac{u^2}{4} \sum_{\sigma_i} \int d z P_{\sigma_1\sigma_2}(z) P_{\sigma_3\sigma_4}(z), \quad (29)$$

where  $z = (\tau, \mathbf{r})$ . From Eqs. (17) to (19) we find that only the product of Kohn anomalies contains slowly oscillating terms on the scale  $v_F/\beta$ , where  $\beta$  stands for the characteristic spin splitting at the Fermi surface

where  $a_B$  is the effective Bohr radius. The weak coupling regime corresponds to high densities such that  $k_F a_B \gg 1$  or  $g \ll 1$ .

Then Eq. (33) can be represented in the following form:

$$\Omega^{(2)} = L_D \frac{v_F^{D+1}}{2^{D+2}} \sum_{\sigma_i} \int_{S_{D-1}} d\mathbf{n}_r \times |M_{\sigma_1\sigma_2}(\mathbf{n}_r)M_{\sigma_3\sigma_4}(-\mathbf{n}_r)|^2 |\Delta_{\sigma_3\sigma_4}^{\sigma_1\sigma_2}(\mathbf{n}_r)|^{D+1}, \quad (36)$$

$$L_D = \frac{g^2}{32} \left(\frac{2}{\pi v_F}\right)^D \frac{\Gamma^2(\frac{D}{2})}{\Gamma(D+2) \cos(\frac{\pi D}{2})}. \quad (37)$$

We perform the summation over the band indexes  $\sigma_i$  explicitly

$$\Omega^{(2)} = L_D \int_{S_{D-1}} d\mathbf{n} \{ |M_{+-}(\mathbf{n})M_{+-}(-\mathbf{n})|^2 |\beta(\mathbf{n}) - \beta(-\mathbf{n})|^{D+1} + |M_{++}(\mathbf{n})M_{--}(\mathbf{n})|^2 |\beta(\mathbf{n}) + \beta(-\mathbf{n})|^{D+1} + 2[|M_{++}(\mathbf{n})M_{-+}(\mathbf{n})|^2 + |M_{--}(\mathbf{n})M_{+-}(\mathbf{n})|^2] |\beta(\mathbf{n})|^{D+1} \}. \quad (38)$$

Here we dropped the index  $\mathbf{r}$  in  $\mathbf{n}_r$ , such that  $\mathbf{n}$  can be also interpreted as the unit vector  $\mathbf{n}_p = \mathbf{p}/p$ ,  $p \approx k_F$ , in the momentum space. This interpretation makes sense because the asymptotics of the Green's function, see Eq. (12), comes from small vicinities of two points on the Fermi surface whose outward normals are collinear with  $\mathbf{r}$ . So,  $\mathbf{r}$  and  $\mathbf{p}$  are in a way pinned to each other.

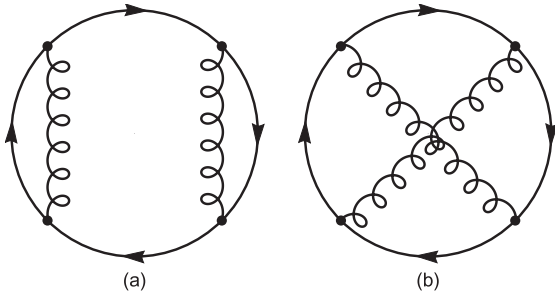


FIG. 2. Other second-order diagrams that do not contribute to the nonanalyticities in  $\Omega$ , see Eqs. (39) and (40).

Finally, we have to check that the second-order diagrams in Figs. 2(a) and 2(b) do not contribute to the nonanalytic terms in  $\Omega$ :

$$\Omega_a = \frac{u^2}{2} \sum_{\sigma_i} \int dz \text{Tr} \{ G_{\sigma_1}^{(0)}(0) G_{\sigma_2}^{(0)}(z) G_{\sigma_3}^{(0)}(0) G_{\sigma_4}^{(0)}(-z) \}, \quad (39)$$

$$\Omega_b = \frac{u^2}{4} \sum_{\sigma_i} \int dz \text{Tr} \{ G_{\sigma_1}^{(0)}(z) G_{\sigma_2}^{(0)}(-z) G_{\sigma_3}^{(0)}(z) G_{\sigma_4}^{(0)}(-z) \}. \quad (40)$$

Here  $G_{\sigma}^{(0)}(0) = G_{\sigma}^{(0)}(\tau = -0, \mathbf{r} = 0)$  due to the ordering of the field operators within the interaction Hamiltonian

$$G_{\sigma}^{(0)}(0) = \int \frac{d\mathbf{p}}{(2\pi)^D} \theta(k_{\sigma}(\mathbf{n}_p) - p) |\sigma, \mathbf{n}_p\rangle \langle \sigma, \mathbf{n}_p|, \quad (41)$$

where  $|\sigma, \mathbf{n}_p\rangle$  are the eigenvectors of the single-particle Hamiltonian, see Eq. (5), and  $k_{\sigma}(\mathbf{n}_p)$  is given by Eq. (9).

The diagram  $\Omega_a$  has a single particle-hole bubble in it due to the Green's functions  $G_{\sigma_2}^{(0)}(z)$  and  $G_{\sigma_4}^{(0)}(-z)$ , see Eq. (39). The product of these Green's functions contains weakly oscillating terms and  $\approx 2k_F$  harmonics. As in the case of  $\Omega^{(1)}$ , the  $2k_F$  harmonics do not produce any nonanalyticities. The weakly oscillating terms originate from the Landau damping part of the particle-hole bubble but these terms vanish due to the integral over  $\tau$ :

$$\int_{-\infty}^{\infty} \frac{d\tau}{(v_F \tau \pm i\tau)^2} = 0. \quad (42)$$

The diagram  $\Omega_b$  is more complicated. Let us consider two matrix products  $G_{\sigma_1}^{(0)}(z)G_{\sigma_2}^{(0)}(-z)$  and  $G_{\sigma_3}^{(0)}(z)G_{\sigma_4}^{(0)}(-z)$ , spin traces are not taken here. As usual, we are after the slowly oscillating terms in Eq. (40). One possibility for this is the product of the forward scattering contributions coming from  $G_{\sigma_1}^{(0)}(z)G_{\sigma_2}^{(0)}(-z)$  and  $G_{\sigma_3}^{(0)}(z)G_{\sigma_4}^{(0)}(-z)$ . From Eq. (12) it is clear that the forward-scattering contributions are nonzero only if  $\sigma_1 = \sigma_2$  and  $\sigma_3 = \sigma_4$ , the matrix products of corresponding projectors vanish otherwise. However, in this case the oscillating factors are canceled exactly, and thus, this contribution is analytic. Another way to obtain slowly oscillating terms in Eq. (40) is the product of the Kohn anomalies contained in  $G_{\sigma_1}^{(0)}(z)G_{\sigma_2}^{(0)}(-z)$  and  $G_{\sigma_3}^{(0)}(z)G_{\sigma_4}^{(0)}(-z)$ . In this case, we have to look at the spin trace in Eq. (40) which is nonzero only if  $\sigma_1 = \sigma_4$  and  $\sigma_2 = \sigma_3$ . This condition becomes obvious if we notice

that the product of the Kohn anomalies of  $G_{\sigma_1}^{(0)}(z)G_{\sigma_2}^{(0)}(-z)$  and  $G_{\sigma_3}^{(0)}(z)G_{\sigma_4}^{(0)}(-z)$  is actually equivalent to the product of the forward-scattering contributions of  $G_{\sigma_2}^{(0)}(-z)G_{\sigma_3}^{(0)}(z)$  and  $G_{\sigma_4}^{(0)}(-z)G_{\sigma_1}^{(0)}(z)$ , which is analytic for the reasons we discussed above.

Hence, only the diagram in Fig. 1(b) contains nonanalytic terms, and therefore, Eq. (38) describes the nonanalytic corrections to  $\Omega$  due to arbitrary spin splitting  $\beta(\mathbf{p})$  within second-order perturbation theory.

Even though Eq. (38) is true in arbitrary number  $D$  of spatial dimensions, we give explicit expressions for  $D = 2$  and  $D = 3$ . For 2DEG the coefficient  $L_2$  is negative, see Eq. (37) for  $D = 2$ :

$$L_2 = -\frac{g^2}{48\pi^2 v_F^2}. \quad (43)$$

The integral over  $d\mathbf{n}$  can be parametrized by a single angle  $\phi \in (0, 2\pi]$ , so the nonanalytic correction Eq. (38) for 2DEG then reads

$$\begin{aligned} \Omega^{(2)} = & -\frac{g^2}{24\pi v_F^2} \int_0^{2\pi} \frac{d\phi}{2\pi} \{ |M_{+-}(\phi)M_{-+}(\phi)|^2 |\beta(\phi) \\ & - \beta(\phi + \pi)|^3 + |M_{++}(\phi)M_{--}(\phi)|^2 |\beta(\phi) \\ & + \beta(\phi + \pi)|^3 + 2[|M_{++}(\phi)M_{-+}(\phi)|^2 \\ & + |M_{--}(\phi)M_{+-}(\phi)|^2] |\beta(\phi)|^3 \}, \quad D = 2. \quad (44) \end{aligned}$$

Our result Eq. (44) agrees with previous studies [44,56,57] and extends them to the case of arbitrary spin splitting. Equation (44) together with Eq. (8) for the matrix elements allows one to find the nonanalytic terms in  $\Omega$  directly from the spin splitting  $\beta(\mathbf{n})$ .

The case of  $D = 3$  is marginal because the non-analytic terms in Eq. (38) are proportional to the fourth power of the spin splitting. The nonanalyticity itself comes from the divergence of the  $L_D$  prefactor at  $D = 3$ , see Eq. (37), which results in an additional logarithm. This is best seen from the dimensional regularization

$$D = 3 - \delta, \quad \delta \rightarrow +0. \quad (45)$$

The dimension  $D$  enters Eq. (38) in the following form:

$$L_D \Delta^{D+1} = -\frac{g^2 \Delta^4}{192\pi^3 v_F^3} \left( \frac{1}{\delta} - \ln \Delta \right) + \mathcal{O}(\delta), \quad (46)$$

where  $\Delta$  takes one of the following values:  $\Delta = |\beta(\mathbf{n}) \pm \beta(-\mathbf{n})|$  or  $\Delta = |\beta(\mathbf{n})|$ . Here we expanded the expression at  $\delta \rightarrow +0$ . The divergent  $1/\delta$  contribution is actually analytic and can be represented by  $\ln \Lambda$  factor,  $\Lambda \sim E_F$ , which compensates the physical dimension of  $\Delta$ :

$$L_D \Delta^{D+1} \rightarrow \frac{g^2}{48\pi^2 v_F^3} \frac{\Delta^4}{4\pi} \ln \left| \frac{\Delta}{\Lambda} \right|, \quad \Lambda \sim E_F. \quad (47)$$

Using the regularization Eq. (47), we find the nonanalytic correction to the spin-split 3DEG

$$\begin{aligned} \Omega^{(2)} = & \frac{g^2}{48\pi^2 v_F^3} \int_{S_2} \frac{dn}{4\pi} \left\{ |M_{+-}(\mathbf{n})M_{-+}(\mathbf{n})|^2 |\beta(\mathbf{n}) - \beta(-\mathbf{n})|^4 \ln \left| \frac{\beta(\mathbf{n}) - \beta(-\mathbf{n})}{\Lambda} \right| \right. \\ & + |M_{++}(\mathbf{n})M_{--}(\mathbf{n})|^2 |\beta(\mathbf{n}) + \beta(-\mathbf{n})|^4 \ln \left| \frac{\beta(\mathbf{n}) + \beta(-\mathbf{n})}{\Lambda} \right| \\ & \left. + 2[|M_{++}(\mathbf{n})M_{-+}(\mathbf{n})|^2 + |M_{--}(\mathbf{n})M_{+-}(\mathbf{n})|^2] |\beta(\mathbf{n})|^4 \ln \left| \frac{\beta(\mathbf{n})}{\Lambda} \right| \right\}, \quad \Lambda \sim E_F, \quad D = 3. \end{aligned} \quad (48)$$

Here, integration over the unit sphere  $S_2$  means  $d\mathbf{n} = \sin\phi_1 d\phi_1 d\phi_2$ ,  $\phi_1 \in [0, \pi]$ ,  $\phi_2 \in (0, 2\pi]$ . The nonanalytic correction is negatively defined for arbitrary spin splitting due to the logarithms. In particular, if  $\beta(\mathbf{n}) = \mathbf{B}$ , we get the well-known result, see Ref. [44],

$$\Omega^{(2)} = \frac{g^2 B^4}{3\pi^2 v_F^3} \ln \left| \frac{2B}{\Lambda} \right|, \quad \Lambda \sim E_F. \quad (49)$$

## VI. LARGE SO SPLITTING AND SMALL MAGNETIC FIELD

Here, we consider the important special case of arbitrary SO splitting and small magnetic field

$$\beta(\mathbf{n}_p) = \beta_{\text{SO}}(\mathbf{n}_p) + \mathbf{B}, \quad B \ll \beta_{\text{SO}}, \quad (50)$$

where  $\mathbf{n}_p = \mathbf{p}/p$ ,  $p \approx k_F$ ,  $\beta_{\text{SO}}$  is a characteristic value of the SO splitting at the Fermi surface. As any SO splitting respects time reversal symmetry, it has to be an odd vector function of  $\mathbf{n}_p$ :

$$\beta_{\text{SO}}(-\mathbf{n}_p) = -\beta_{\text{SO}}(\mathbf{n}_p). \quad (51)$$

As we consider  $B \ll \beta_{\text{SO}}$ , then we can expand  $\beta(\mathbf{n})$  with respect to  $\mathbf{B}$ :

$$\beta(\mathbf{n}) \approx \beta_{\text{SO}}(\mathbf{n}) + \frac{\beta_{\text{SO}}(\mathbf{n}) \cdot \mathbf{B}}{\beta_{\text{SO}}(\mathbf{n})}, \quad (52)$$

where  $\beta_{\text{SO}}(\mathbf{n}) = |\beta_{\text{SO}}(\mathbf{n})|$ . Together with the symmetry condition Eq. (51), we conclude that only the very first term in Eq. (38) contributes to the nonanalyticity with respect to  $\mathbf{B}$  due to the following identity:

$$\beta(\mathbf{n}) - \beta(-\mathbf{n}) \approx 2 \frac{\beta_{\text{SO}}(\mathbf{n}) \cdot \mathbf{B}}{\beta_{\text{SO}}(\mathbf{n})}. \quad (53)$$

As we only consider the leading nonanalyticity, we calculate the matrix elements at  $\mathbf{B} = 0$ :

$$M_{\sigma\sigma}(\mathbf{n}) = 0, \quad M_{\sigma-\sigma}(\mathbf{n}) = -1. \quad (54)$$

Substituting Eqs. (53) and (54) in Eq. (38), we find the nonanalytic in  $\mathbf{B}$  correction to  $\Omega$  in case of arbitrary SO splitting:

$$\delta\Omega(\mathbf{B}) = L_D \int_{S_{D-1}} dn \left| 2 \frac{\beta_{\text{SO}}(\mathbf{n}) \cdot \mathbf{B}}{\beta_{\text{SO}}(\mathbf{n})} \right|^{D+1}, \quad (55)$$

where  $\delta\Omega(\mathbf{B})$  indicates that only the nonanalytic terms with respect to  $\mathbf{B}$  are included. Thus, we see that the nonanalyticity in magnetic field  $\mathbf{B}$  cannot be eliminated even by arbitrary SO splitting, in contrast to the results of Ref. [58].

The elementary processes that are responsible for the nonanalyticity given by Eq. (55) are shown in Fig. 3. These

processes describe the resonant scattering of a pair of electrons with the band index  $\sigma$  and opposite momenta  $\pm\mathbf{k}_\sigma$  into a pair of electrons in the other band with index  $-\sigma$  and momenta  $\pm\mathbf{k}_{-\sigma}$  that are collinear with momenta of initial electrons  $\pm\mathbf{k}_\sigma$ . The momentum transfer in such a scattering processes is close to  $2k_F$ , see Fig. 3(b). The scattering with small momentum transfer is forbidden due to the orthogonality condition Eq. (6). The considered processes are resonant due to the time-reversal symmetry, see Eq. (51). The collinearity condition comes from the *local nesting* when the momentum transfer between the resonantly scattering states also matches small vicinities around these states. This matching is satisfied when the outward normals in the scattering states are collinear such that the mismatch comes only from different curvatures of the Fermi surface in the considered points. The local nesting strongly enhances the corresponding scattering processes because not only the considered states are in resonance, but also small vicinities of states around them. For example, the Kohn anomaly in the particle-hole bubble is a result of such a local nesting for the states scattering with the  $2k_F$  momentum transfer. The perfect local nesting corresponds to the Landau damping of the particle-hole excitations with energy and momentum around zero, in this case the scattered region in the particle-hole bubble is mapped onto itself.

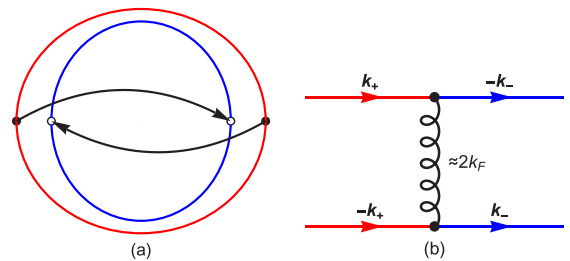


FIG. 3. (a) Fermi surfaces at arbitrary SO splitting, red (blue) color corresponds to  $\sigma = +1$  ( $\sigma = -1$ ). The arrows show the resonant scattering processes. (b) The interaction matrix element corresponding to the resonant scattering processes at finite SO splitting. Here a pair of electrons with the band index  $\sigma = +1$  and opposite momenta  $\pm\mathbf{k}_+$  scatter into a pair with momenta  $\pm\mathbf{k}_-$  that are collinear with  $\pm\mathbf{k}_+$ . These processes are resonant due to the time reversal symmetry, see Eq. (51). The collinearity of  $\mathbf{k}_+$  and  $\mathbf{k}_-$  is due to the *local nesting* discussed in the main text after Eq. (55). These processes are responsible for the nonanalyticity in  $\Omega$  with respect to small magnetic field  $\mathbf{B}$ , see Eq. (55).

It is also instructive to write down Eq. (55) for 2DEG and 3DEG explicitly

$$\delta\Omega(\mathbf{B}) = -\frac{g^2|\mathbf{B}|^3}{3\pi v_F^2} \int_0^{2\pi} \frac{d\phi}{2\pi} \left| \frac{\boldsymbol{\beta}_{SO}(\phi) \cdot \mathbf{b}}{\beta_{SO}(\phi)} \right|^3, \quad D = 2, \quad (56)$$

$$\delta\Omega(\mathbf{B}) = \frac{g^2 B^4}{3\pi^2 v_F^3} \ln \left| \frac{2B}{\Lambda} \int_{S_2} \frac{d\mathbf{n}}{4\pi} \left| \frac{\boldsymbol{\beta}_{SO}(\mathbf{n}) \cdot \mathbf{b}}{\beta_{SO}(\mathbf{n})} \right|^4 \right|, \quad D = 3, \quad (57)$$

where  $\mathbf{b} = \mathbf{B}/B$  is the unit vector along  $\mathbf{B}$ . We neglected the term  $\ln |\boldsymbol{\beta}_{SO}(\mathbf{n}) \cdot \mathbf{b}/\beta_{SO}(\mathbf{n})|$  in Eq. (57) because it just slightly renormalizes the regular  $B^4$  term. Here it is convenient to introduce the angular form-factor  $F_D(\mathbf{b})$  which depends on the direction  $\mathbf{b}$  of the magnetic field and on the SO splitting

$$F_D(\mathbf{b}) = \int_{S_{D-1}} \frac{d\mathbf{n}}{S_{D-1}} \left| \frac{\boldsymbol{\beta}_{SO}(\mathbf{n}) \cdot \mathbf{b}}{\beta_{SO}(\mathbf{n})} \right|^{D+1}, \quad (58)$$

where  $S_{D-1}$  is the area of a unit  $(D-1)$ -dimensional sphere.

The form-factors  $F_D(\mathbf{b})$  can only be positive or zero, see Eq. (58). If we demand  $F_D(\mathbf{b}) = 0$  for any unit vector  $\mathbf{b}$ , it is equivalent to say that  $\boldsymbol{\beta}_{SO}(\mathbf{n}) \cdot \mathbf{b} = 0$  for any  $\mathbf{b}$  and also  $\beta_{SO}(\mathbf{n}) \neq 0$  from Eq. (50). As this is clearly impossible, we conclude that  $F_D(\mathbf{b})$  can never vanish for all unit vectors  $\mathbf{b}$  even at arbitrary SO splitting  $\boldsymbol{\beta}_{SO}(\mathbf{n})$ . Therefore, the nonanalyticity with respect to  $\mathbf{B}$  cannot be cut by any SO splitting neither in 2DEG nor in 3DEG.

Nevertheless, the SO splitting is important because it leads to strong anisotropy of the nonanalytic term, see Eq. (55), which is described by the form-factor  $F_D(\mathbf{b})$ . If we extrapolate this result to the vicinity of a FQPT, we conclude that the direction of spontaneous magnetization must coincide with

the maximum of  $F_D(\mathbf{b})$ . In particular, we predict a first-order Ising FQPT in electron gas with a general SO splitting which breaks the spin rotational symmetry down to  $\mathbb{Z}_2$ .

## VII. NONANALYTIC CORRECTION IN 2DEG WITH RASHBA AND DRESSELHAUS SOI

In this section we give an example of 2DEG with Rashba and Dresselhaus SO splittings:

$$\boldsymbol{\beta}_{SO}(\phi) = [(\alpha_D + \alpha_R)k_F \sin \phi, (\alpha_D - \alpha_R)k_F \cos \phi, 0], \quad (59)$$

where the  $x$  and  $y$  axes correspond to the  $[110]$  and  $[\bar{1}\bar{1}0]$  crystallographic directions and  $\alpha_R$  and  $\alpha_D$  are the Rashba and the Dresselhaus coupling constants, respectively. The qualitative picture of the SO-split Fermi surfaces is shown in Fig. 3(a). It is more convenient to introduce the following SO couplings:

$$a_{\pm} \equiv (\alpha_R \pm \alpha_D)k_F. \quad (60)$$

Then we find the angular form-factor  $F_2(\mathbf{b})$ , see Eqs. (56) and (58)

$$F_2(\mathbf{b}) = \int_0^{2\pi} \frac{d\phi}{2\pi} \frac{|a_+ b_x \sin \phi - a_- b_y \cos \phi|^3}{(a_+^2 \sin^2 \phi + a_-^2 \cos^2 \phi)^{\frac{3}{2}}}, \quad (61)$$

where  $\mathbf{b} = \mathbf{B}/B$  is the unit vector along  $\mathbf{B}$ . We want to identify the directions  $\mathbf{b}^*$  where  $F_2(\mathbf{b}^*)$  is maximal. It is clear that all such directions have  $b_z^* = 0$ . Then  $b_x^*$  and  $b_y^*$  can be parametrized by a single angle  $\Psi$ :

$$b_x^* = \cos \Psi, \quad b_y^* = \sin \Psi. \quad (62)$$

The integral in Eq. (61) is quite cumbersome but elementary:

$$\begin{aligned} \frac{\pi}{2} F_2(\zeta, \Psi) = & -\frac{\zeta \cos(2\Psi)}{\zeta^2 - 1} + \frac{\zeta \cos \Psi}{(\zeta^2 - 1)^{\frac{3}{2}}} (\zeta^2 \cos^2 \Psi - 3 \sin^2 \Psi) \arctan(\sqrt{\zeta^2 - 1} \cos \Psi) \\ & + \frac{\sin \Psi}{(\zeta^2 - 1)^{\frac{3}{2}}} (\sin^2 \Psi - 3\zeta^2 \cos^2 \Psi) \ln \left( \frac{\sqrt{\zeta^2 \cos^2 \Psi + \sin^2 \Psi}}{\sqrt{\zeta^2 - 1} \sin \Psi + \zeta} \right), \quad \zeta \equiv \left| \frac{a_+}{a_-} \right| = \left| \frac{\alpha_R + \alpha_D}{\alpha_R - \alpha_D} \right| > 1. \end{aligned} \quad (63)$$

We added  $\zeta$  as additional argument of  $F_2(\mathbf{b})$  for convenience. Equation (63) is true only if  $\zeta > 1$ . If  $\zeta < 1$ , we use the

following identity:

$$F_2(\zeta, \Psi) = F_2\left(\frac{1}{\zeta}, \frac{\pi}{2} - \Psi\right). \quad (64)$$

The form-factor  $F_2(\zeta, \Psi)$  is plotted in Fig. 4. In case of  $\zeta = 1$  the form factor is independent of  $\Psi$ ,  $F_2(1, \Psi) = 4/(3\pi)$ . This corresponds to the case of either pure Rashba or pure Dresselhaus SO splitting. In either case the ferromagnetic ground state is an easy-plane ferromagnet predicted in Refs. [56,57].

In case both SO interactions are present, i.e.,  $\zeta \neq 1$ , the form factor is a nontrivial function of the angle  $\Psi$ , see Fig. 4. The extremal values of the  $\pi$ -periodic function  $F_2(\zeta, \Psi)$  correspond to  $\Psi = 0$  and  $\Psi = \pi/2$ :

$$F_2(\zeta, 0) = \frac{2}{\pi} \left[ \frac{\zeta^3 \arctan(\sqrt{\zeta^2 - 1})}{(\zeta^2 - 1)^{\frac{3}{2}}} - \frac{\zeta}{\zeta^2 - 1} \right], \quad (65)$$

$$F_2\left(\zeta, \frac{\pi}{2}\right) = \frac{2}{\pi} \left[ \frac{\zeta}{\zeta^2 - 1} - \frac{\ln(\zeta + \sqrt{\zeta^2 - 1})}{(\zeta^2 - 1)^{\frac{3}{2}}} \right], \quad (66)$$

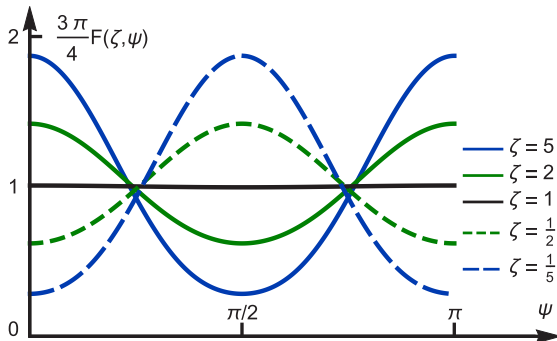


FIG. 4. The form-factor  $F_2(\zeta, \Psi)$  (multiplied by  $3\pi/4$ ), see Eq. (63), as a function of  $\Psi \in (0, \pi)$  for different values of  $\zeta$ .



where  $\zeta > 1$ . It is straightforward to see that at  $\zeta > 1$  the maximum of  $F_2(\zeta, \Psi)$  corresponds to  $\Psi = 0$ . If  $\zeta < 1$ , we use Eq. (64) and find that the maximum corresponds to  $\Psi = \pi/2$ , see also Fig. 4.

If these calculations are extrapolated to the vicinity of the FQPT, we predict an Ising ferromagnetism in 2DEG with Rashba and Dresselhaus SO splitting. The direction of spontaneous magnetization here coincides with the spin quantization axis of the states that are maximally split by the SO coupling, namely, along [110] ([1 $\bar{1}$ 0]) if  $\alpha_R$  and  $\alpha_D$  have the same (opposite) signs. The easy-plane ferromagnet is only realized when either Rashba or Dresselhaus SO splitting is zero.

### VIII. SPIN SUSCEPTIBILITY IN THE PARAMAGNETIC PHASE

The nonanalytic corrections destabilizing the FQCP separating ferromagnetic and paramagnetic phases can be measured experimentally via the magnetic-field dependence of the spin susceptibility  $\chi_{ij}(\mathbf{B})$  in the paramagnetic phase

$$\chi_{ij}(\mathbf{B}) = -\frac{\partial^2 \Omega(\mathbf{B})}{\partial B_i \partial B_j}. \quad (67)$$

Deep inside the paramagnetic phase where  $g \ll 1$  or  $\lambda_F \ll a_B$ , see Eq. (35), the nonanalytic correction is given by Eqs. (56) and (57), so the corresponding nonanalytic corrections to the spin susceptibility are the following:

$$\delta \chi_{ij}(\mathbf{B}) = \frac{2g^2 |B|}{\pi v_F^2} \kappa_{ij}^{(2)}(\mathbf{b}), \quad D = 2, \quad (68)$$

$$\delta \chi_{ij}(\mathbf{B}) = -\frac{4g^2 B^2}{\pi^2 v_F^3} \ln \left| \frac{2B}{\Lambda} \right| \kappa_{ij}^{(3)}(\mathbf{b}), \quad D = 3, \quad (69)$$

$$\kappa_{ij}^{(D)}(\mathbf{b}) = \int_{S_{D-1}} \frac{dn}{S_{D-1}} \left| \frac{\beta_{\text{SO}}(\mathbf{n}) \cdot \mathbf{b}}{\beta_{\text{SO}}(\mathbf{n})} \right|^{D-1} \frac{\beta_{\text{SO}}^i(\mathbf{n}) \beta_{\text{SO}}^j(\mathbf{n})}{\beta_{\text{SO}}^2(\mathbf{n})}, \quad (70)$$

where  $\Lambda \sim E_F$ ,  $\beta_{\text{SO}}^i(\mathbf{n})$  is the  $i$ th component of the vector  $\beta_{\text{SO}}(\mathbf{n})$ . These results are valid for  $B \gg T$ . In the opposite regime  $B \ll T$ , the nonanalyticity is regularized by the temperature. An important feature here is the nontrivial angular dependence of the spin susceptibility on  $\mathbf{b}$  due to the SO splitting, see the angular tensor  $\kappa_{ij}^{(D)}(\mathbf{b})$ . Notice the following identity:

$$\kappa_{ij}^{(D)}(\mathbf{b}) b_i b_j = F_D(\mathbf{b}), \quad (71)$$

where  $F_D(\mathbf{b})$  is the form factor introduced in Eq. (58). Thus, the form factor  $F_D(\mathbf{b})$  can be retrieved from a spin susceptibility measurement. Moreover, the directions corresponding to the maxima of the form factor  $F_D(\mathbf{b})$  are the preferred directions of the net magnetization in the magnetically ordered phase. To measure local spin susceptibility one can use, for example, ultrasensitive nitrogen-vacancy center based detectors [66].

### IX. CONCLUSION

In this paper we revisited FQPT in interacting clean 2DEG and 3DEG with arbitrary SO splitting. First, we calculated nonanalytic corrections to the thermodynamic potential  $\Omega$

with respect to arbitrary spin splitting in second order with respect to electron-electron interaction. So far, this has been done in the literature only for very limited number of special cases [44,56–58]. Here we generalized the calculation for arbitrary spin splitting and arbitrary spatial dimension  $D > 1$ , see Eq. (38). First, we see that even arbitrarily complex SO splitting is not able to cut the nonanalyticity in  $\Omega$  with respect to the magnetic field, see Eq. (55). This is a direct consequence of the backscattering processes shown in Fig. 3. Such processes were not taken into account in Ref. [58] where a complicated-enough SO splitting is predicted to cut the nonanalyticity. Second, the nonanalytic correction is strongly anisotropic and follows the symmetry of the SO splitting. This results in reduced symmetry of the ferromagnetic ground state. For example, the ferromagnetic ground state in the Rashba 2DEG is the easy-plane ferromagnet. If both Rashba and Dresselhaus terms are present, the symmetry of the ferromagnetic ground state is reduced down to the in-plane easy-axis (Ising) ferromagnet. Strong anisotropy of the nonanalytic term can be measured via the nonanalytic correction to the spin susceptibility in the paramagnetic phase that is strongly anisotropic and follows the symmetry of the SO splitting. The candidate materials are the pressure-tuned 3D ferromagnets ZrZn<sub>2</sub> [60], UGe<sub>2</sub> [61], and many others [63], or density-tuned 2D quantum wells [62].

### ACKNOWLEDGMENTS

This work was supported by the Georg H. Endress Foundation, the Swiss National Science Foundation (SNSF), and NCCR SPIN. This project received funding from the European Union's Horizon 2020 research and innovation program (ERC Starting Grant, Grant Agreement No. 757725).

### APPENDIX: ASYMPTOTICS OF THE GREEN'S FUNCTION

We start from the Fourier representation of the Green's function

$$G(\tau, \mathbf{r}) = \int \frac{d\mathbf{p}}{(2\pi)^D} e^{i\mathbf{p}\cdot\mathbf{r}} G(\tau, \mathbf{p}), \quad (A1)$$

where  $\tau$  is the imaginary time,  $\mathbf{r}$  a  $D$ -dimensional position vector, and  $\mathbf{p}$  a  $D$ -dimensional momentum vector. Here we do not indicate any band index because it is fixed. The asymptotics at large  $\tau \gg 1/E_F$  and large  $r = |\mathbf{r}| \gg \lambda_F$  is dominated by the vicinity of the Fermi surface  $\mathcal{FS}$ , so we can expand the momentum  $\mathbf{p}$  into the momentum  $\mathbf{k}$  on the Fermi surface  $\mathcal{FS}$  and the momentum along the outward normal  $\mathbf{n}(\mathbf{k})$  at  $\mathbf{k}$ , see Fig. 5(a),

$$\mathbf{p} = \mathbf{k} + \mathbf{n}(\mathbf{k}) \delta p, \quad \mathbf{k} \in \mathcal{FS}, \quad (A2)$$

where  $\delta p$  is the distance from  $\mathbf{p}$  to the Fermi surface  $\mathcal{FS}$ . Notice that  $\delta p > 0$  ( $\delta p < 0$ ) corresponds to the states above (below) the Fermi surface. At large  $r \gg 1/k_F$ ,  $k_F$  is the typical momentum scale on the Fermi surface, we have  $\delta p \sim 1/r \ll k_F$ , so we can approximate the integral over  $\mathbf{p}$  by the integration over a thin layer around the Fermi

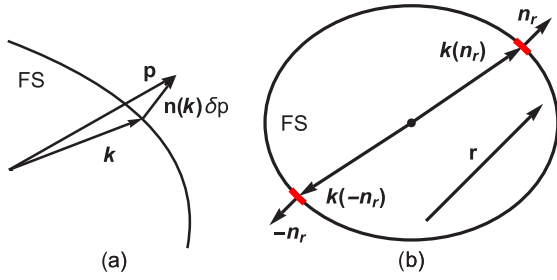


FIG. 5. (a) Expansion of the momentum  $\mathbf{p}$  close to the Fermi surface  $\mathcal{FS}$ :  $\mathbf{k}$  is the normal projection of  $\mathbf{p}$  on  $\mathcal{FS}$ ,  $\delta p \ll k_F$ , see Eq. (A2). (b) Two points  $\mathbf{k}(\mathbf{n}_r)$  and  $\mathbf{k}(-\mathbf{n}_r)$  on a nearly spherical Fermi surface  $\mathcal{FS}$  where the outward normals are equal to  $\mathbf{n}_r$  and  $-\mathbf{n}_r$ , respectively. The two red patches on  $\mathcal{FS}$  correspond to the vicinities of the points  $\mathbf{k}(\pm\mathbf{n}_r)$  which give the leading contribution to the  $\tau \gg 1/E_F$  and  $r \gg \lambda_F$  asymptotics of the Green's function.

surface

$$G(\tau, \mathbf{r}) \approx \int_{-\infty}^{\infty} \frac{d\delta p}{2\pi} \int_{\mathbf{k} \in \mathcal{FS}} \frac{d\mathbf{k}}{(2\pi)^{D-1}} \times e^{i\mathbf{k} \cdot \mathbf{r}} e^{i\delta p \mathbf{n}(\mathbf{k}) \cdot \mathbf{r}} G(\tau, \delta p, \mathbf{k}), \quad (\text{A3})$$

$$G(\tau, \delta p, \mathbf{k}) \equiv G[\tau, \mathbf{k} + \mathbf{n}(\mathbf{k})\delta p]. \quad (\text{A4})$$

Here we extended the integral over  $\delta p$  to the interval  $(-\infty, \infty)$  because the convergence radius of this integral is very short at  $r \rightarrow \infty$ , namely,  $\delta p \sim 1/r$ . Hence, we approximated the initial Fourier transform Eq. (A1) by the integral over the fiber bundle  $\mathcal{FS} \times (-\infty, \infty)$ .

As  $r \rightarrow \infty$ , we can use the stationary phase method to find the asymptotics. First, we evaluate the integral over the Fermi surface. The stationary condition for the phase of the rapidly oscillating factor  $e^{i\mathbf{k} \cdot \mathbf{r}}$  in Eq. (A3) reads

$$d\mathbf{k} \cdot \mathbf{r} = 0, \quad (\text{A5})$$

where  $d\mathbf{k}$  is an arbitrary infinitesimal (but nonzero) element of the tangent space  $\mathcal{T}(\mathbf{k})$  attached to the Fermi surface  $\mathcal{FS}$  at the point  $\mathbf{k}$ . Hence,  $\mathbf{r}$  has to be orthogonal to the whole linear space  $\mathcal{T}(\mathbf{k})$ , which has codimension of one. This means that the stationary phase condition is satisfied at the points  $\mathbf{k}' \in \mathcal{FS}$  where  $\mathbf{r}$  is collinear with the normals  $\mathbf{n}(\mathbf{k}')$ :

$$\mathbf{n}(\mathbf{k}') = s(\mathbf{k}', \mathbf{n}_r) \mathbf{n}_r, \quad \mathbf{n}_r = \frac{\mathbf{r}}{r}, \quad (\text{A6})$$

where  $s(\mathbf{k}', \mathbf{n}_r) = +1$  [ $s(\mathbf{k}', \mathbf{n}_r) = -1$ ] if the outward normal  $\mathbf{n}(\mathbf{k}')$  and the radius vector  $\mathbf{r}$  are parallel (antiparallel). We include all such points  $\mathbf{k}'$  into a set  $\mathcal{P}(\mathbf{n}_r)$ :

$$\mathcal{P}(\mathbf{n}_r) = \{\mathbf{k}' \in \mathcal{FS} | \mathbf{n}(\mathbf{k}') = \pm \mathbf{n}_r\}. \quad (\text{A7})$$

It is clear that  $\mathcal{P}(-\mathbf{n}_r) = \mathcal{P}(\mathbf{n}_r)$  and  $s(\mathbf{k}', -\mathbf{n}_r) = -s(\mathbf{k}', \mathbf{n}_r)$ .

At this point we can take the integral over  $\delta p$  in Eq. (A3)

$$\int_{-\infty}^{\infty} \frac{d\delta p}{2\pi} e^{i\delta p \mathbf{n}(\mathbf{k}') \cdot \mathbf{r}} G(\tau, \delta p, \mathbf{k}') = \mathcal{G}[\tau, s(\mathbf{k}', \mathbf{n}_r) \mathbf{r}, \mathbf{k}'], \quad (\text{A8})$$

where we used that  $\mathbf{k}' \in \mathcal{P}(\mathbf{n}_r)$  and  $s(\mathbf{k}', \mathbf{n}_r) = \mathbf{n}(\mathbf{k}') \cdot \mathbf{n}_r = \pm 1$ , see Eq. (A6). Here  $\mathcal{G}(\tau, x, \mathbf{k})$  is the 1D Fourier transform

of the Green function:

$$\mathcal{G}(\tau, x, \mathbf{k}) = \int_{-\infty}^{\infty} \frac{d\delta p}{2\pi} e^{i\delta p x} G(\tau, \delta p, \mathbf{k}), \quad \mathbf{k} \in \mathcal{FS}. \quad (\text{A9})$$

Note that such a one-dimensional (1D) Fourier transform is generally dependent on the point  $\mathbf{k} \in \mathcal{FS}$ . Substituting this into Eq. (A3), we find

$$G(\tau, \mathbf{r}) \approx \sum_{\mathbf{k}' \in \mathcal{P}(\mathbf{n}_r)} e^{i\mathbf{k}' \cdot \mathbf{r}} J_{\mathbf{k}'}(r) \mathcal{G}[\tau, s(\mathbf{k}', \mathbf{n}_r) \mathbf{r}, \mathbf{k}'], \quad (\text{A10})$$

$$J_{\mathbf{k}'}(r) = \int_{\mathbf{k} \in \mathcal{FS}} \frac{d\mathbf{k}}{(2\pi)^{D-1}} e^{i(\mathbf{k}-\mathbf{k}') \cdot \mathbf{r}}. \quad (\text{A11})$$

The function  $J_{\mathbf{k}'}(r)$  appears due to the integration over a small vicinity of a point  $\mathbf{k}' \in \mathcal{P}(\mathbf{n}_r)$ .

The integral  $J_{\mathbf{k}'}(r)$  converges due to the finite curvature of the Fermi surface at  $\mathbf{k}'$ . This is true even if the interaction is very strong such that the Fermi surface becomes critical. To evaluate this integral, it is convenient to introduce an auxiliary function  $\varepsilon(\mathbf{p})$  with the following properties:

$$\varepsilon(\mathbf{p}) = 0 \quad \text{if } \mathbf{p} \in \mathcal{FS}, \quad (\text{A12})$$

$$\mathbf{v}(\mathbf{p}) = \frac{\partial \varepsilon(\mathbf{p})}{\partial \mathbf{p}} \neq 0 \quad \text{if } \mathbf{p} \in \mathcal{FS}. \quad (\text{A13})$$

We notice here that there are infinitely many choices for such a function, but we will show that the result is independent of the choice. In the case of a free electron gas the natural choice for  $\varepsilon(\mathbf{p})$  is the electron dispersion. The condition Eq. (A13) is required to generate the outward normal  $\mathbf{n}(\mathbf{k})$  at each point  $\mathbf{k} \in \mathcal{FS}$ :

$$\mathbf{v}(\mathbf{k}) = v(\mathbf{k}) \mathbf{n}(\mathbf{k}), \quad \mathbf{k} \in \mathcal{FS}. \quad (\text{A14})$$

Here  $v(\mathbf{k}) > 0$  for all  $\mathbf{k} \in \mathcal{FS}$ .

Consider two close points  $\mathbf{k} \in \mathcal{FS}$  and  $\mathbf{k}' \in \mathcal{FS}$ . According to Eq. (A12), we can write

$$\varepsilon(\mathbf{k}) = \varepsilon(\mathbf{k}') = 0. \quad (\text{A15})$$

Using the Taylor series expansion, we find

$$0 = \varepsilon(\mathbf{k}) \approx \varepsilon(\mathbf{k}') + (\mathbf{k} - \mathbf{k}') \cdot \mathbf{v}(\mathbf{k}') + \frac{1}{2} (\mathbf{k} - \mathbf{k}')^T R(\mathbf{k}') (\mathbf{k} - \mathbf{k}'), \quad (\text{A16})$$

$$R_{ij}(\mathbf{p}) = \frac{\partial^2 \varepsilon(\mathbf{p})}{\partial p_i \partial p_j}, \quad (\text{A17})$$

where we used the matrix notations in Eq. (A16), and the superscript  $T$  stands for transposition. Substituting Eq. (A14) into Eq. (A16), we find

$$(\mathbf{k} - \mathbf{k}') \cdot \mathbf{n}(\mathbf{k}') \approx -(\mathbf{k} - \mathbf{k}')^T \frac{R(\mathbf{k}')}{2v(\mathbf{k}')} (\mathbf{k} - \mathbf{k}'). \quad (\text{A18})$$

In Eq. (A11)  $\mathbf{k}' \in \mathcal{P}(\mathbf{n}_r)$ , so  $\mathbf{n}(\mathbf{k}')$  satisfies Eq. (A6). This allows us to write

$$(\mathbf{k} - \mathbf{k}') \cdot \mathbf{r} \approx -s(\mathbf{k}', \mathbf{n}_r) r (\mathbf{k} - \mathbf{k}')^T \frac{R(\mathbf{k}')}{2v(\mathbf{k}')} (\mathbf{k} - \mathbf{k}'). \quad (\text{A19})$$

The expression is quadratic with respect to the small difference  $\mathbf{k} - \mathbf{k}'$ . At large  $r$  the convergence radius of the integral  $J_{\mathbf{k}'}(r)$  scales as  $|\mathbf{k} - \mathbf{k}'| \propto 1/\sqrt{r}$ , so we indeed have to integrate over a small vicinity of  $\mathbf{k}' \in \mathcal{P}(\mathbf{n}_r)$  and the Taylor

expansion is valid. Equation (A19) also shows that the component of  $\mathbf{k} - \mathbf{k}'$  along the normal  $\mathbf{n}(\mathbf{k}')$  is only quadratic with respect to  $\mathbf{k} - \mathbf{k}'$ , so at a given accuracy we can approximate  $\mathbf{k} - \mathbf{k}'$  on the right-hand side of Eq. (A19) by its orthogonal projection onto the tangent space  $\mathcal{T}(\mathbf{k}')$ :

$$J_{\mathbf{k}'}(r) \approx \int_{\kappa \in \mathcal{T}(\mathbf{k}')} \frac{d\kappa}{(2\pi)^{D-1}} e^{-irs(\mathbf{k}', \mathbf{n}_r) \kappa^T A(\mathbf{k}') \kappa}, \quad (\text{A20})$$

$$A(\mathbf{k}') = \frac{R_{\mathcal{T}}(\mathbf{k}')}{2v(\mathbf{k}')}, \quad (\text{A21})$$

where  $R_{\mathcal{T}}(\mathbf{k}')$  is the restriction of the tensor  $R(\mathbf{k}')$  to the tangent space  $\mathcal{T}(\mathbf{k}')$ . We reduced the initial integral  $J_{\mathbf{k}'}(r)$  to a standard Gaussian integral

$$J_{\mathbf{k}'}(r) \approx \left( \frac{1}{4\pi r} \right)^{\frac{D-1}{2}} \frac{e^{-i\frac{\pi}{4}s(\mathbf{k}', \mathbf{n}_r) \mathfrak{S}[A(\mathbf{k}')]} }{\sqrt{|\det A(\mathbf{k}')|}}, \quad (\text{A22})$$

$$\mathfrak{S}[A(\mathbf{k}')] = \sum_{i=1}^{D-1} \text{sgn}(a_i), \quad (\text{A23})$$

where  $a_i$  are all  $D - 1$  eigenvalues of the symmetric matrix  $A(\mathbf{k}')$ . In all cases that we consider in this paper  $\det A(\mathbf{k}') \neq 0$  at any point  $\mathbf{k} \in \mathcal{FS}$ . In other words, we consider only Fermi surfaces with nonzero Gauss curvature at each point.

Let us check that the matrix  $A(\mathbf{k})$ ,  $\mathbf{k} \in \mathcal{FS}$ , is indeed independent of the choice of  $\varepsilon(\mathbf{p})$ . For this, we consider another parametrization

$$\tilde{\varepsilon}(\mathbf{p}) = f(\mathbf{p})\varepsilon(\mathbf{p}), \quad (\text{A24})$$

where  $f(\mathbf{p})$  is an arbitrary smooth function such that  $f(\mathbf{p}) > 0$ . As  $f(\mathbf{p}) \neq 0$ , then  $\tilde{\varepsilon}(\mathbf{p}) = 0$  if and only if  $\varepsilon(\mathbf{p}) = 0$ , i.e.,  $\tilde{\varepsilon}(\mathbf{p}) = 0$  defines the Fermi surface  $\mathcal{FS}$ . Let us find the velocity  $\tilde{v}(\mathbf{k})$  when  $\mathbf{k} \in \mathcal{FS}$ :

$$\tilde{v}(\mathbf{k})\mathbf{n}(\mathbf{k}) = \frac{\partial \tilde{\varepsilon}(\mathbf{k})}{\partial \mathbf{k}} = \frac{\partial f(\mathbf{k})}{\partial \mathbf{k}} \varepsilon(\mathbf{k}) + f(\mathbf{k})v(\mathbf{k})\mathbf{n}(\mathbf{k}), \quad (\text{A25})$$

where  $v(\mathbf{k})$  is defined in Eqs. (A13) and (A14). As  $\mathbf{k} \in \mathcal{FS}$ , then  $\varepsilon(\mathbf{k}) = 0$ , so we find

$$\tilde{v}(\mathbf{k}) = f(\mathbf{k})v(\mathbf{k}) > 0, \quad \mathbf{k} \in \mathcal{FS}. \quad (\text{A26})$$

Similarly, we can calculate the tensor  $\tilde{R}(\mathbf{k})$ ,  $\mathbf{k} \in \mathcal{FS}$ :

$$\begin{aligned} \tilde{R}_{ij}(\mathbf{k}) &= \frac{\partial^2 \tilde{\varepsilon}(\mathbf{k})}{\partial k_i \partial k_j} = f(\mathbf{k})R_{ij}(\mathbf{k}) \\ &+ v(\mathbf{k}) \left( \frac{\partial f}{\partial k_i} \mathbf{n}_j(\mathbf{k}) + \frac{\partial f}{\partial k_j} \mathbf{n}_i(\mathbf{k}) \right), \quad \mathbf{k} \in \mathcal{FS}, \end{aligned} \quad (\text{A27})$$

where  $R_{ij}(\mathbf{k})$  is defined in Eq. (A17). The second line in Eq. (A27) contains a term which vanishes in all products  $\kappa^T \tilde{R}(\mathbf{k}) \kappa$  where  $\kappa \in \mathcal{T}(\mathbf{k})$ , i.e.,  $\kappa \cdot \mathbf{n}(\mathbf{k}) = 0$ . This means that the restriction to the tangent space  $\mathcal{T}(\mathbf{k})$  is especially simple

$$\tilde{R}_{\mathcal{T}}(\mathbf{k}) = f(\mathbf{k})R_{\mathcal{T}}(\mathbf{k}), \quad \mathbf{k} \in \mathcal{FS}. \quad (\text{A28})$$

Using Eqs. (A26) and (A28), we indeed find that the operator  $\tilde{A}(\mathbf{k})$ ,  $\mathbf{k} \in \mathcal{FS}$ , is invariant with respect to different choices of  $\varepsilon(\mathbf{p})$ :

$$\tilde{A}(\mathbf{k}) = \frac{\tilde{R}_{\mathcal{T}}(\mathbf{k})}{2\tilde{v}(\mathbf{k})} = \frac{R_{\mathcal{T}}(\mathbf{k})}{2v(\mathbf{k})} = A(\mathbf{k}), \quad \mathbf{k} \in \mathcal{FS}. \quad (\text{A29})$$

All in all, the long-range asymptotics of the Green's function of an interacting Fermi gas is the following:

$$G(\tau, \mathbf{r}) \approx \sum_{\mathbf{k}' \in \mathcal{P}(\mathbf{n}_r)} \frac{C(\mathbf{k}', \mathbf{n}_r)}{(4\pi r)^{\frac{D-1}{2}}} e^{i\mathbf{k}' \cdot \mathbf{r}} \mathcal{G}[\tau, s(\mathbf{k}', \mathbf{n}_r)r, \mathbf{k}'], \quad (\text{A30})$$

$$C(\mathbf{k}', \mathbf{n}_r) = \frac{e^{-i\frac{\pi}{4}s(\mathbf{k}', \mathbf{n}_r) \mathfrak{S}[A(\mathbf{k}')]} }{\sqrt{|\det A(\mathbf{k}')|}}. \quad (\text{A31})$$

This is the general result which is suitable for a Fermi surface of arbitrary geometry. The matrix structure is hidden in  $\mathcal{G}[\tau, s(\mathbf{k}', \mathbf{n}_r)r, \mathbf{k}']$ . Next, we give examples for spherical or nearly spherical Fermi surfaces.

### 1. Spherical Fermi surface

The simplest example is the spherical Fermi surface with the Fermi momentum  $k_F$ . We considered this case in Ref. [59]. For an arbitrary direction  $\mathbf{n}_r$  there are exactly two points on the Fermi surface whose normals are collinear with  $\mathbf{n}_r$ , see Fig. 5(b),

$$\mathcal{P}(\mathbf{n}_r) = \{\pm k_F \mathbf{n}_r\}. \quad (\text{A32})$$

In this case, the sum over  $\mathbf{k}'$  in Eq. (A30) contains only two terms, namely,  $\mathbf{k}' = \pm k_F \mathbf{n}_r$ . To calculate the matrix  $A(\mathbf{k}')$ , we consider the function

$$\varepsilon(\mathbf{p}) = \frac{p^2 - k_F^2}{2}. \quad (\text{A33})$$

The velocity  $v(\mathbf{p})$  and the tensor  $R(\mathbf{p})$  are then the following:

$$v(\mathbf{p}) = p, \quad (\text{A34})$$

$$R_{ij}(\mathbf{p}) = \delta_{ij}. \quad (\text{A35})$$

This allows us to identify the matrix  $A(\mathbf{k})$ ,  $|\mathbf{k}| = k_F$ :

$$A(\mathbf{k}) = \frac{I}{2k_F}, \quad |\mathbf{k}| = k_F, \quad (\text{A36})$$

where  $I$  is the  $(D - 1) \times (D - 1)$  identity matrix on the tangent space  $\mathcal{T}(\mathbf{k})$ . Substituting this into Eq. (A30), we find the asymptotics of the Green's function in the case of the spherical Fermi surface

$$\begin{aligned} G(\tau, \mathbf{r}) &\approx \left( \frac{1}{\lambda_F r} \right)^{\frac{D-1}{2}} [e^{i(k_F r - \vartheta)} \mathcal{G}(\tau, r) \\ &+ e^{-i(k_F r - \vartheta)} \mathcal{G}(\tau, -r)], \end{aligned} \quad (\text{A37})$$

$$\vartheta = \frac{\pi}{4}(D - 1), \quad (\text{A38})$$

$$\mathcal{G}(\tau, x) = \int_{-\infty}^{\infty} \frac{d\delta p}{2\pi} e^{i\delta p x} G(\tau, \delta p), \quad (\text{A39})$$

where  $\lambda_F = 2\pi/k_F$  is the Fermi wavelength. Here we also used the spherical symmetry, i.e.,  $G(\tau, \mathbf{p}) = G(\tau, p)$ , so  $G(\tau, \delta p, \mathbf{k})$  is independent of  $\mathbf{k} \in \mathcal{FS}$ .

### 2. Nearly spherical Fermi surface

Here we consider another example when the Fermi surface is nearly spherical and can be modeled by the following

dispersion:

$$\varepsilon(\mathbf{p}) = \frac{p^2 - k_F^2}{2m} - \beta(\mathbf{p}). \quad (\text{A40})$$

We denote points on the Fermi surface  $\mathcal{FS}$  by  $\mathbf{k}$ , they satisfy the equation  $\varepsilon(\mathbf{k}) = 0$ :

$$k^2 = k_F^2 + 2m\beta(\mathbf{k}). \quad (\text{A41})$$

In this part we make the following assumptions about the smooth function  $\beta(\mathbf{p})$ :

$$|\beta(\mathbf{k})| \ll E_F, \quad \nabla\beta(\mathbf{k}) \equiv \left. \frac{\partial\beta(\mathbf{p})}{\partial\mathbf{p}} \right|_{\mathbf{p}=\mathbf{k}} \ll v_F, \quad (\text{A42})$$

where  $\mathbf{k} \in \mathcal{FS}$ ,  $2E_F = k_F v_F$  is the Fermi energy and  $v_F = k_F/m$  the Fermi velocity. Using the first condition in Eq. (A42), we find the approximate Fermi surface equation

$$k(\mathbf{e}) \approx k_F + \frac{\beta(\mathbf{e})}{v_F}, \quad k(\mathbf{e})\mathbf{e} \in \mathcal{FS}, \quad (\text{A43})$$

where  $\mathbf{e}$  is an arbitrary unit vector and  $\beta(\mathbf{e})$  stands for  $\beta(k_F\mathbf{e})$ .

The outward normal  $\mathbf{n}(\mathbf{k})$  at  $\mathbf{k} \in \mathcal{FS}$  is defined through the gradient of  $\varepsilon(\mathbf{p})$  at  $\mathbf{p} = \mathbf{k}$ :

$$v(\mathbf{k})\mathbf{n}(\mathbf{k}) = \frac{\mathbf{k}}{m} - \nabla\beta(\mathbf{k}), \quad (\text{A44})$$

$$v^2(\mathbf{k}) = \frac{k^2}{m^2} - 2\frac{\mathbf{k} \cdot \nabla\beta(\mathbf{k})}{m} + [\nabla\beta(\mathbf{k})]^2, \quad (\text{A45})$$

where the second equation here is just the first one squared. Here is where we use the second condition in Eq. (A42). In

linear order in  $\beta(\mathbf{k})$  we find

$$v(\mathbf{k}) \approx \frac{k(\mathbf{n})}{m} - \mathbf{n} \cdot \nabla\beta(\mathbf{n}), \quad (\text{A46})$$

$$\mathbf{k} \cdot \mathbf{n}(\mathbf{k}) \approx k(\mathbf{n}) = k_F + \frac{\beta(\mathbf{n})}{v_F}, \quad (\text{A47})$$

where  $\beta(\mathbf{n})$  stands for  $\beta(k_F\mathbf{n})$ .

We are only interested in the points  $\mathbf{k}' \in \mathcal{FS}$  with normals  $\mathbf{n}(\mathbf{k}') = s\mathbf{n}_r$ ,  $s = \pm 1$ , see Fig. 5(b). Using Eq. (A47), we find the oscillating phase

$$\mathbf{k}' \cdot \mathbf{r} = sr\mathbf{k}' \cdot \mathbf{n}(\mathbf{k}') \approx sk(\mathbf{n}_r)r, \quad (\text{A48})$$

where we used Eq. (A47). Neglecting the weak dependence of the prefactor  $C(\mathbf{k}', \mathbf{n}_r)$  on  $\beta(\mathbf{k}')$ , see Eq. (A31), we find the asymptotic behavior of the Green's function in the case of a nearly spherical Fermi surface

$$G(\tau, \mathbf{r}) \approx \left( \frac{1}{\lambda_F r} \right)^{\frac{D-1}{2}} [e^{i[k(\mathbf{n}_r)r - \vartheta]} \mathcal{G}(\tau, r) + e^{-i[k(-\mathbf{n}_r)r - \vartheta]} \mathcal{G}(\tau, -r)], \quad (\text{A49})$$

where  $k(\mathbf{n})$  is given by Eq. (A43) and  $\vartheta$  by Eq. (A38). Here,  $\mathcal{G}(\tau, x)$  is calculated at  $\beta(\mathbf{p}) = 0$ , i.e., it coincides with the spherically symmetric case. Importantly, the oscillatory factors  $e^{\pm ik(\pm\mathbf{n}_r)r}$  in Eq. (A49) depend explicitly on  $\beta(\pm\mathbf{n}_r)$ , which is crucial for the resonant scattering processes near the Fermi surface.

- 
- [1] A. P. Ramirez, *J. Phys.: Condens. Matter* **9**, 8171 (1997).  
[2] J. M. D. Coey, M. Viret, and S. von Molnár, *Adv. Phys.* **48**, 167 (1999).  
[3] K. Ghosh, C. J. Lobb, R. L. Greene, S. G. Karabashev, D. A. Shulyatev, A. A. Arsenov, and Y. Mukovskii, *Phys. Rev. Lett.* **81**, 4740 (1998).  
[4] D. Kim, B. Revaz, B. L. Zink, F. Hellman, J. J. Rhyne, and J. F. Mitchell, *Phys. Rev. Lett.* **89**, 227202 (2002).  
[5] T. Dietl, H. Ohno, F. Matsukura, J. Cibert, and D. Ferrand, *Science* **287**, 1019 (2000).  
[6] H. Ohno, H. Munekata, T. Penney, S. von Molnár, and L. L. Chang, *Phys. Rev. Lett.* **68**, 2664 (1992).  
[7] H. Ohno, D. Chiba, F. Matsukura, T. Omiya, E. Abe, T. Dietl, Y. Ohno, and K. Ohtani, *Nature (London)* **408**, 944 (2000).  
[8] S. Tongay, S. S. Varnoosfaderani, B. R. Appleton, J. Wu, and A. F. Hebard, *Appl. Phys. Lett.* **101**, 123105 (2012).  
[9] M. Bonilla, S. Kolekar, Y. Ma, H. C. Diaz, V. Kalappattil, R. Das, T. Eggers, H. R. Gutierrez, M.-H. Phan, and M. Batzill, *Nat. Nanotechnol.* **13**, 289 (2018).  
[10] J. G. Roch, G. Froehlicher, N. Leisgang, P. Makk, K. Watanabe, T. Taniguchi, and R. J. Warburton, *Nat. Nanotechnol.* **14**, 432 (2019).  
[11] J. G. Roch, D. Miserev, G. Froehlicher, N. Leisgang, L. Sponfeldner, K. Watanabe, T. Taniguchi, J. Klinovaja, D. Loss, and R. J. Warburton, *Phys. Rev. Lett.* **124**, 187602 (2020).  
[12] K. Hao, R. Shreiner, A. Kindseth, and A. A. High, *Sci. Adv.* **8**, eabq7650 (2022).  
[13] Y. L. Huang, W. Chen, and A. T. S. Wee, *SmartMat* **2**, 139 (2021).  
[14] B. T. Matthias and R. M. Bozorth, *Phys. Rev.* **109**, 604 (1958).  
[15] F. R. de Boer, C. J. Schinkel, J. Biesterbos, and S. Proost, *J. Appl. Phys.* **40**, 1049 (1969).  
[16] S. Takagi, H. Yasuoka, J. L. Smith, and C. Y. Huang, *J. Magn. Magn. Mater.* **31-34**, 273 (1983).  
[17] R. Nakabayashi, Y. Tazuki, and S. Murayama, *J. Phys. Soc. Jpn.* **61**, 774 (1992).  
[18] H.-J. Deiseroth, K. Aleksandrov, C. Reiner, L. Kienle, and R. K. Kremer, *Eur. J. Inorg. Chem.* **2006**, 1561 (2006).  
[19] F. Al Ma'Mari, T. Moorsom, G. Teobaldi, W. Deacon, T. Prokscha, H. Luetkens, S. Lee, G. E. Sterbinsky, D. A. Arena, D. A. MacLaren, M. Flokstra, M. Ali, M. C. Wheeler, G. Burnell, B. J. Hickey, and O. Cespedes, *Nature (London)* **524**, 69 (2015).  
[20] X. Xu, Y. W. Li, S. R. Duan, S. L. Zhang, Y. J. Chen, L. Kang, A. J. Liang, C. Chen, W. Xia, Y. Xu, P. Malinowski, X. D. Xu, J.-H. Chu, G. Li, Y. F. Guo, Z. K. Liu, L. X. Yang, and Y. L. Chen, *Phys. Rev. B* **101**, 201104(R) (2020).  
[21] J. Walter, B. Voigt, E. Day-Roberts, K. Heltemes, R. M. Fernandes, T. Birol, and C. Leighton, *Sci. Adv.* **6**, eabb7721 (2020).  
[22] C. Zener, *Phys. Rev.* **82**, 403 (1951).

- [23] A. S. Alexandrov and A. M. Bratkovsky, *Phys. Rev. Lett.* **82**, 141 (1999).
- [24] J. A. Vergés, V. Martín-Mayor, and L. Brey, *Phys. Rev. Lett.* **88**, 136401 (2002).
- [25] E. C. Stoner, *Proc. R. Soc. A* **165**, 372 (1938).
- [26] E. C. Stoner, *Proc. R. Soc. A* **169**, 339 (1939).
- [27] V. L. Ginzburg and L. D. Landau, *On the theory of superconductivity* (Springer, Berlin, Heidelberg, 2009), doi:10.1007/978-3-540-68008-6\_4.
- [28] K. G. Wilson and J. Kogut, *Phys. Rep.* **12**, 75 (1974).
- [29] J. A. Hertz, *Phys. Rev. B* **14**, 1165 (1976).
- [30] A. J. Millis, *Phys. Rev. B* **48**, 7183 (1993).
- [31] S. Sachdev, *Phys. Rev. B* **55**, 142 (1997).
- [32] T. Vojta, D. Belitz, R. Narayanan, and T. R. Kirkpatrick, *Z. Phys. B: Condens. Matter* **103**, 451 (1997).
- [33] D. Belitz, T. R. Kirkpatrick, and T. Vojta, *Phys. Rev. B* **55**, 9452 (1997).
- [34] D. Belitz, T. R. Kirkpatrick, and T. Vojta, *Phys. Rev. Lett.* **82**, 4707 (1999).
- [35] A. V. Chubukov and D. L. Maslov, *Phys. Rev. B* **68**, 155113 (2003).
- [36] A. V. Chubukov and D. L. Maslov, *Phys. Rev. B* **69**, 121102(R) (2004).
- [37] D. Belitz, T. R. Kirkpatrick, and J. Rollbühler, *Phys. Rev. Lett.* **93**, 155701 (2004).
- [38] D. Belitz, T. R. Kirkpatrick, and J. Rollbühler, *Phys. Rev. Lett.* **94**, 247205 (2005).
- [39] H. V. Löhneysen, A. Rosch, M. Vojta, and P. Wölfle, *Rev. Mod. Phys.* **79**, 1015 (2007).
- [40] D. Belitz, T. R. Kirkpatrick, and T. Vojta, *Rev. Mod. Phys.* **77**, 579 (2005).
- [41] S. Coleman and E. Weinberg, *Phys. Rev. D* **7**, 1888 (1973).
- [42] B. I. Halperin, T. C. Lubensky, and S.-K. Ma, *Phys. Rev. Lett.* **32**, 292 (1974).
- [43] D. L. Maslov, A. V. Chubukov, and R. Saha, *Phys. Rev. B* **74**, 220402(R) (2006).
- [44] D. L. Maslov and A. V. Chubukov, *Phys. Rev. B* **79**, 075112 (2009).
- [45] A. Abanov, A. V. Chubukov, and J. Schmalian, *Adv. Phys.* **52**, 119 (2003).
- [46] B. Tanatar and D. M. Ceperley, *Phys. Rev. B* **39**, 5005 (1989).
- [47] F. Rapisarda and G. Senatore, *Aust. J. Phys.* **49**, 161 (1996).
- [48] D. Varsano, S. Moroni, and G. Senatore, *Europhys. Lett.* **53**, 348 (2001).
- [49] C. Attacalite, S. Moroni, P. Gori-Giorgi, and G. B. Bachelet, *Phys. Rev. Lett.* **88**, 256601 (2002).
- [50] D. M. Ceperley and B. J. Alder, *Phys. Rev. Lett.* **45**, 566 (1980).
- [51] G. Ortiz, M. Harris, and P. Ballone, *Phys. Rev. Lett.* **82**, 5317 (1999).
- [52] F. H. Zong, C. Lin, and D. M. Ceperley, *Phys. Rev. E* **66**, 036703 (2002).
- [53] P.-F. Loos and P. M. W. Gill, *WIREs Comput. Mol. Sci.* **6**, 410 (2016).
- [54] T. Baldsiefen, A. Cangì, F. G. Eich, and E. K. U. Gross, *Phys. Rev. A* **96**, 062508 (2017).
- [55] M. Holzmann and S. Moroni, *Phys. Rev. Lett.* **124**, 206404 (2020).
- [56] R. A. Žak, D. L. Maslov, and D. Loss, *Phys. Rev. B* **82**, 115415 (2010).
- [57] R. A. Žak, D. L. Maslov, and D. Loss, *Phys. Rev. B* **85**, 115424 (2012).
- [58] T. R. Kirkpatrick and D. Belitz, *Phys. Rev. Lett.* **124**, 147201 (2020).
- [59] D. Miserev, J. Klinovaja, and D. Loss, *Phys. Rev. B* **103**, 075104 (2021).
- [60] M. Uhlarz, C. Pfeiderer, and S. M. Hayden, *Phys. Rev. Lett.* **93**, 256404 (2004).
- [61] V. Taufour, D. Aoki, G. Knebel, and J. Flouquet, *Phys. Rev. Lett.* **105**, 217201 (2010).
- [62] M. S. Hossain, M. K. Ma, K. A. Villegas Rosales, Y. J. Chung, L. N. Pfeiffer, K. W. West, K. W. Baldwin, and M. Shayegan, *Proc. Natl. Acad. Sci. USA* **117**, 32244 (2020).
- [63] M. Brando, D. Belitz, F. M. Grosche, and T. R. Kirkpatrick, *Rev. Mod. Phys.* **88**, 025006 (2016).
- [64] J. M. Luttinger, *J. Math. Phys.* **4**, 1154 (1963).
- [65] S. Lounis, P. Zahn, A. Weismann, M. Wenderoth, R. G. Ulbrich, I. Mertig, P. H. Dederichs, and S. Blügel, *Phys. Rev. B* **83**, 035427 (2011).
- [66] P. Stano, J. Klinovaja, A. Yacoby, and D. Loss, *Phys. Rev. B* **88**, 045441 (2013).